Dual elimination of the glucagon and GLP-1 receptors in mice reveals plasticity in the incretin axis

Safina Ali,[1,2] Benjamin J. Lamont,[2] Maureen J. Charron,[3] and Daniel J. Drucker[1,2]

[1]Department of Laboratory Medicine and Pathobiology and [2]Department of Medicine, Samuel Lunenfeld Research Institute, Mt. Sinai Hospital, University of Toronto, Toronto, Ontario, Canada. [3]Department of Biochemistry, Albert Einstein College of Medicine, New York, New York, USA.

Disordered glucagon secretion contributes to the symptoms of diabetes, and reduced glucagon action is known to improve glucose homeostasis. In mice, genetic deletion of the glucagon receptor (*Gcgr*) results in increased levels of the insulinotropic hormone glucagon-like peptide 1 (GLP-1), which may contribute to the alterations in glucose homeostasis observed in *Gcgr*$^{-/-}$ mice. Here, we assessed the contribution of GLP-1 receptor (GLP-1R) signaling to the phenotype of *Gcgr*$^{-/-}$ mice by generating *Gcgr*$^{-/-}$*Glp1r*$^{-/-}$ mice. Although insulin sensitivity was similar in all genotypes, fasting glucose was increased in *Gcgr*$^{-/-}$*Glp1r*$^{-/-}$ mice. Elimination of the *Glp1r* normalized gastric emptying and impaired intraperitoneal glucose tolerance in *Gcgr*$^{-/-}$ mice. Unexpectedly, deletion of *Glp1r* in *Gcgr*$^{-/-}$ mice did not alter the improved oral glucose tolerance and increased insulin secretion characteristic of that genotype. Although *Gcgr*$^{-/-}$*Glp1r*$^{-/-}$ islets exhibited increased sensitivity to the incretin glucose-dependent insulinotropic polypeptide (GIP), mice lacking both *Glp1r* and the GIP receptor (*Gipr*) maintained preservation of the enteroinsular axis following reduction of Gcgr signaling. Moreover, *Gcgr*$^{-/-}$*Glp1r*$^{-/-}$ islets expressed increased levels of the cholecystokinin A receptor (*Cckar*) and G protein–coupled receptor 119 (*Gpr119*) mRNA transcripts, and *Gcgr*$^{-/-}$*Glp1r*$^{-/-}$ mice exhibited increased sensitivity to exogenous CCK and the GPR119 agonist AR231453. Our data reveal extensive functional plasticity in the enteroinsular axis via induction of compensatory mechanisms that control nutrient-dependent regulation of insulin secretion.

Introduction

Glucagon, a 29-amino-acid peptide hormone, is produced in pancreatic α cells and, together with insulin, plays a key role in regulating hepatic glucose production, serving as the first line of defense against hypoglycemia (1). Disordered control of glucagon secretion is observed in type 2 diabetes mellitus (T2DM) (2–4) and together with insulin deficiency or resistance results in metabolic derangements characteristic of T2DM (5). Glucagon exerts its actions through a class B family G protein–coupled receptor (GPCR), the glucagon receptor (Gcgr), that is expressed not only in the liver, but in a broad range of tissues, including the heart, kidney, endocrine pancreas, and the central nervous system (6–10).

The observations that inappropriately increased levels of glucagon promote increased hepatic glucose production and hyperglycemia (3, 11–14) have fostered efforts targeting suppression of glucagon action for the treatment of T2DM (15). Reduction of glucagon activity using glucagon antagonists, immunoneutralizing antisera, or antisense oligonucleotides (ASOs) directed against Gcgr attenuates hyperglycemia in experimental models of diabetes (16–23). The importance of glucagon action has also been examined via generation and characterization of the *Gcgr*$^{-/-}$ mouse. Surprisingly, mice with complete germline disruption of Gcgr are viable and grow normally (24, 25). *Gcgr*$^{-/-}$ mice exhibit normal body weight, food intake, and energy expenditure, yet display improved glucose tolerance, enhanced β cell function and insulin sensitivity, resistance to streptozotocin-induced (STZ-induced) diabetes, and delayed gastric emptying (25–27). These favorable phenotypes support reduction of glucagon action for the therapy of T2DM.

Interpretation of metabolic derangements arising from loss of Gcgr signaling is complicated by the concomitant finding of markedly increased circulating levels of glucagon-like peptide 1 (GLP-1) in *Gcgr*$^{-/-}$ mice (25). GLP-1, a related proglucagon-derived peptide normally secreted from enteroendocrine L cells, produces many of the actions described in *Gcgr*$^{-/-}$ mice. The increased circulating levels of GLP-1 in *Gcgr*$^{-/-}$ mice likely reflect increased production of bioactive GLP-1 in the *Gcgr*$^{-/-}$ pancreas (25). As GLP-1 improves β cell function and glucose tolerance, reduces gastric emptying, and promotes islet cell proliferation and resistance to STZ-induced diabetes, attribution of precise mechanisms responsible for the improved metabolic phenotype in *Gcgr*$^{-/-}$ mice is challenging. We now demonstrate that a functional GLP-1 receptor (GLP-1R) is essential for control of fasting and ambient glycemia, enhancement of glucose-stimulated insulin secretion following i.p. glucose challenge, and inhibition of gastric emptying in *Gcgr*$^{-/-}$ mice. Unexpectedly, *Gcgr*$^{-/-}$*Glp1r*$^{-/-}$ mice continued to exhibit improved oral glucose tolerance and enhanced β cell function despite loss of two key insulinotropic β cell receptors. Although loss of GLP-1 action is classically compensated for by upregulation of the other major incretin, glucose-dependent insulinotropic polypeptide (GIP) (28), we demonstrate that reduction of Gcgr expression in mice with combined inactivation of both

Conflict of interest: D.J. Drucker has been an advisor or consultant for Amylin Pharmaceuticals, Arena Pharmaceuticals Inc., Arisaph Pharmaceuticals Inc., Eli Lilly Inc., GlaxoSmithKline, Hoffman LaRoche Inc., Merck Research Laboratories, Metabolex Inc., Novartis Pharmaceuticals, Novo Nordisk Inc., and Transition Pharmaceuticals Inc.

Citation for this article: *J Clin Invest* doi:10.1172/JCI43615.

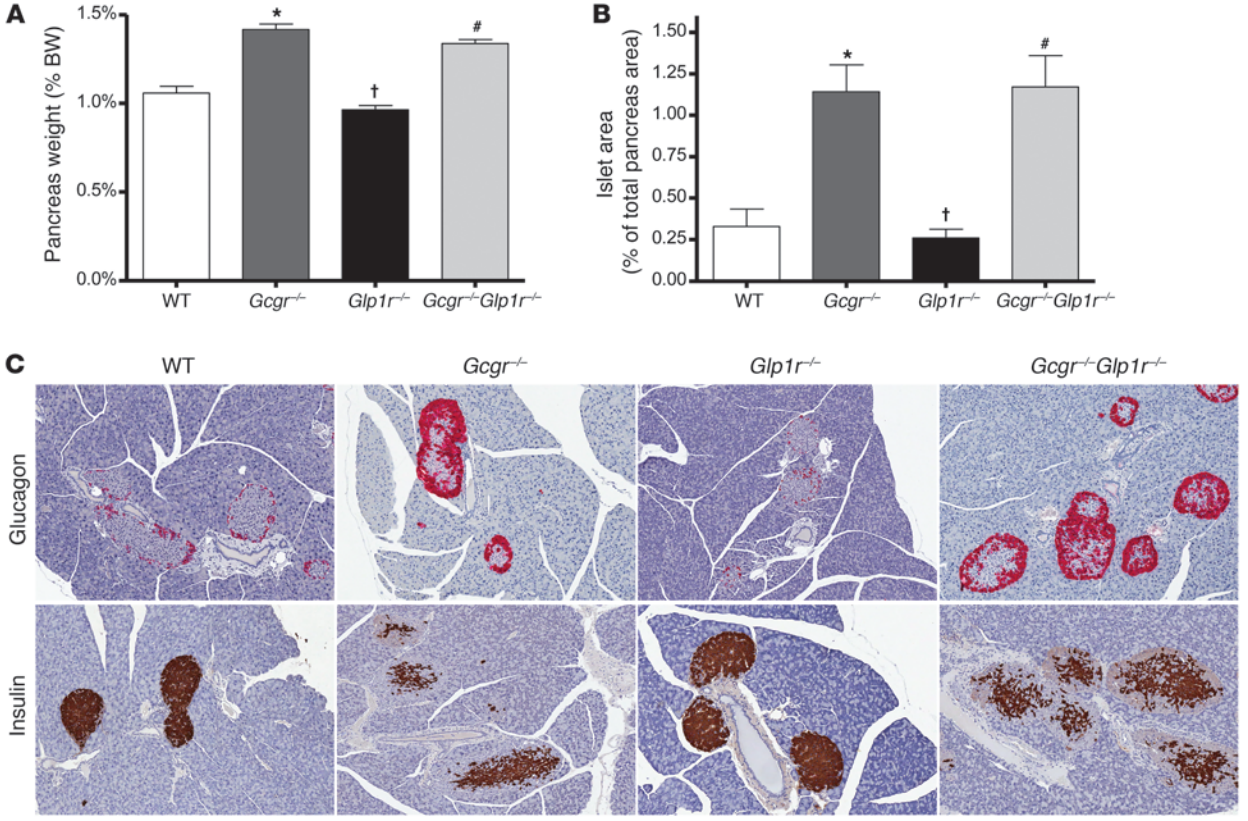

Figure 1
Glp1r is not required for development of increased pancreas weight or α cell hyperplasia in *Gcgr*$^{-/-}$ mice. (**A**) Pancreas weight of 20- to 24-week-old mice shown as percentage of the final body weight (n = 7–20 mice per group). (**B**) Islet area shown as a percentage of total pancreas area (n = 4–12 mice per group) (**C**) Representative histological sections of pancreas stained for insulin or glucagon alone. Final magnification, ×80. Values are expressed as mean ± SEM. *P < 0.05, *Gcgr*$^{-/-}$ mice versus WT littermate controls; #P < 0.05, *Gcgr*$^{-/-}$*Glp1r*$^{-/-}$ mice versus WT littermate control mice; †P < 0.05, *Glp1r*$^{-/-}$ versus *Gcgr*$^{-/-}$*Glp1r*$^{-/-}$ mice.

Glp1r and the GIP receptor (*Gipr*) genes continues to be associated with preservation of oral glucose tolerance and enhanced insulin secretion. Disruption of the classical (GLP-1R and GIPR) enteroinsular axis was associated with enhanced expression and activity of the cholecystokinin A receptor (*Cckar*) and G protein–coupled receptor 119 (*Gpr119*), functionally related insulinotropic receptors that respond to nutrient-sensitive signals. These findings reveal considerable plasticity in the incretin-related mechanisms regulating β cell function and glucose homeostasis.

Results

Glp1r is not required for pancreas enlargement or α cell hyperplasia in Gcgr$^{-/-}$ *mice.* Body weight, food intake, physical activity, and energy expenditure were comparable in WT, single incretin receptor knockout, and *Gcgr*$^{-/-}$*Glp1r*$^{-/-}$ mice (Supplemental Figure 1; supplemental material available online with this article; doi:10.1172/JCI43615DS1). As *Gcgr*$^{-/-}$ mice exhibit increased pancreatic mass and marked islet and α cell hyperplasia (25) and GLP-1R activation promotes expansion of islet and pancreatic mass (29–31), we assessed the contribution of Glp1r to the development of these abnormalities in *Gcgr*$^{-/-}$ mice. Consistent with previous findings, *Gcgr*$^{-/-}$ mice exhibited very high circulating levels of GLP-1 (Supplemental Figure 2A), significantly increased pancreas weight, and an approximately 4-fold increase in islet area (Figure 1); however, islet area and pancreatic mass remained significantly increased to a similar extent in *Gcgr*$^{-/-}$*Glp1r*$^{-/-}$ mice (Figure 1, A and B). Immunohistochemical analysis revealed that the increased islet area was predominantly due to α cell hyperplasia, with most *Gcgr*$^{-/-}$ and *Gcgr*$^{-/-}$*Glp1r*$^{-/-}$ islets containing a core of β cells surrounded by an expanded mantle of hyperplastic α cells (Figure 1C). Hence, Glp1r is not required for development of increased pancreatic mass and islet hyperplasia following loss of Gcgr action.

Disruption of Glp1r leads to increased fasting glycemia in Gcgr$^{-/-}$ *mice.* Both fasting and random glucose were reduced in *Gcgr*$^{-/-}$ mice (Figure 2, A and B), consistent with the central role of glucagon in the maintenance of euglycemia (25). Basal GLP-1R signaling also regulates fasting glycemia (32), classically through suppression of glucagon secretion (33). Surprisingly, a significant increase in fasting glucose was observed in *Gcgr*$^{-/-}$*Glp1r*$^{-/-}$ compared with *Gcgr*$^{-/-}$ mice (Figure 2A) and elimination of the Glp1r normalized random-fed glycemia in *Gcgr*$^{-/-}$*Glp1r*$^{-/-}$ mice (Figure 2B). Hence, loss of Glp1r substantially attenuates improvements in both ambient and fasting glycemia in *Gcgr*$^{-/-}$ mice (25).

Elimination of Glp1r reverses improvements in i.p. glucose tolerance in Gcgr$^{-/-}$ *mice.* To elucidate the contribution of enhanced GLP-1

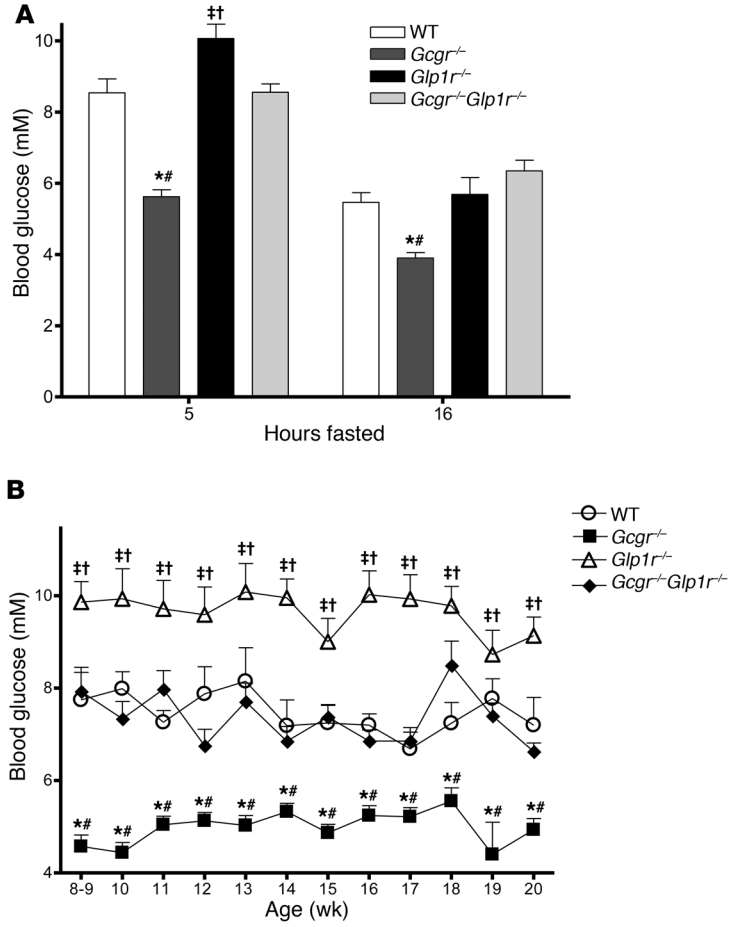

Figure 2
Glp1r controls fasting and fed glycemia in *Gcgr*$^{-/-}$ mice. (**A**) Blood glucose following 5 or 16 hours of fasting in 8- to 12-week-old WT, *Gcgr*$^{-/-}$, *Glp1r*$^{-/-}$, and *Gcgr*$^{-/-}$*Glp1r*$^{-/-}$ mice (n = 5–30 mice per genotype). (**B**) Weekly random-fed blood glucose levels in 8- to 20-week-old *Gcgr*$^{-/-}$*Glp1r*$^{-/-}$, *Gcgr*$^{-/-}$, *Glp1r*$^{-/-}$, and littermate control WT mice (n = 3–20 mice per group). Values are expressed as mean ± SEM. $^{*}P < 0.05$, *Gcgr*$^{-/-}$ versus *Gcgr*$^{-/-}$*Glp1r*$^{-/-}$ mice; $^{\#}P < 0.05$, *Gcgr*$^{-/-}$ versus WT mice; $^{\ddagger}P < 0.05$, *Glp1r*$^{-/-}$ versus WT mice; $^{\dagger}P < 0.05$, *Glp1r*$^{-/-}$ versus *Gcgr*$^{-/-}$*Glp1r*$^{-/-}$ mice.

receptor signaling to improved β cell function and glucose tolerance in *Gcgr*$^{-/-}$ mice (25), we first assessed clearance of i.p. glucose in mice of different genotypes. Intraperitoneal glucose tolerance was significantly enhanced and plasma insulin levels increased in *Gcgr*$^{-/-}$ mice; conversely, i.p. glucose tolerance was impaired in *Glp1r*$^{-/-}$ mice (Figure 3A), consistent with previous studies (25, 32). Furthermore, disruption of Glp1r in *Gcgr*$^{-/-}$ mice reversed the improvements in i.p. glucose tolerance and normalized plasma insulin levels in *Gcgr*$^{-/-}$*Glp1r*$^{-/-}$ mice (Figure 3, A and B), whereas insulin sensitivity, approximated by insulin tolerance, was comparable among all genotypes (Figure 3C). Hence, the elevated levels of GLP-1 leading to increased GLP-1R signaling is primarily responsible for enhanced β cell function and improved glucose clearance after i.p. glucose challenge in *Gcgr*$^{-/-}$ mice.

The GLP-1 receptor mediates reduced gastric emptying; however, oral glucose tolerance remains improved independent of Glp1r in Gcgr$^{-/-}$ *mice.* As GLP-1–mediated reduction in gastric emptying may substantially account for the improved oral glucose tolerance in *Gcgr*$^{-/-}$ mice (25, 26), we quantified gastric emptying with two complementary methods. Both liquid-phase gastric emptying, assessed via measurement of plasma acetaminophen levels, and solid-phase gastric emptying were significantly reduced in *Gcgr*$^{-/-}$ mice and normalized in *Gcgr*$^{-/-}$*Glp1r*$^{-/-}$ mice (Figure 4, A and B). We hypothesized that normalization of gastric emptying would be associated with deterioration of oral glucose tolerance in *Gcgr*$^{-/-}$*Glp1r*$^{-/-}$ mice (25). Unexpectedly, oral glucose tolerance remained significantly improved in *Gcgr*$^{-/-}$*Glp1r*$^{-/-}$ mice to an extent comparable to that in *Gcgr*$^{-/-}$ mice alone (Figure 4, C and D). Furthermore, in contrast to the normalization of plasma insulin levels seen following i.p. glucose challenge in *Gcgr*$^{-/-}$*Glp1r*$^{-/-}$ versus *Gcgr*$^{-/-}$ mice (Figure 3B), *Gcgr*$^{-/-}$*Glp1r*$^{-/-}$ mice continued to exhibit significantly increased levels of plasma insulin following oral glucose challenge (Figure 4D).

Islets from Gcgr$^{-/-}$*Glp1r*$^{-/-}$ *mice display increased sensitivity to GIP.* As *Glp1r*$^{-/-}$ mice exhibit enhanced GIP secretion and increased sensitivity to GIP (28), we explored whether GIP-related mechanisms underlie the enhanced enteral glucose-stimulated insulin secretion in *Gcgr*$^{-/-}$*Glp1r*$^{-/-}$ mice. Although levels of GIP were modestly elevated in *Glp1r*$^{-/-}$ mice, GIP levels were not significantly increased in *Gcgr*$^{-/-}$*Glp1r*$^{-/-}$ mice (Supplemental Figure 2B). We next examined control of insulin secretion from WT, *Glp1r*$^{-/-}$, *Gcgr*$^{-/-}$, and *Gcgr*$^{-/-}$*Glp1r*$^{-/-}$ islets. No significant differences across genotypes were detected in response to 16.7 mM glucose with a modest but nonsignificant reduction in insulin secretion observed with *Gcgr*$^{-/-}$*Glp1r*$^{-/-}$ islets (Figure 5A). Consistent with the loss of the Glp1r, the insulinotropic response to exendin-4 was absent in *Glp1r*$^{-/-}$ and *Gcgr*$^{-/-}$*Glp1r*$^{-/-}$ islets (Figure 5A). Although GIP sensitivity was not enhanced in *Glp1r*$^{-/-}$ or *Gcgr*$^{-/-}$ islets, the insulinotropic response to GIP was significantly increased in *Gcgr*$^{-/-}$*Glp1r*$^{-/-}$ islets (Figure 5A).

To explore the selectivity of the enhanced response to GIP, we tested a range of other insulin secretagogues. In contrast to the

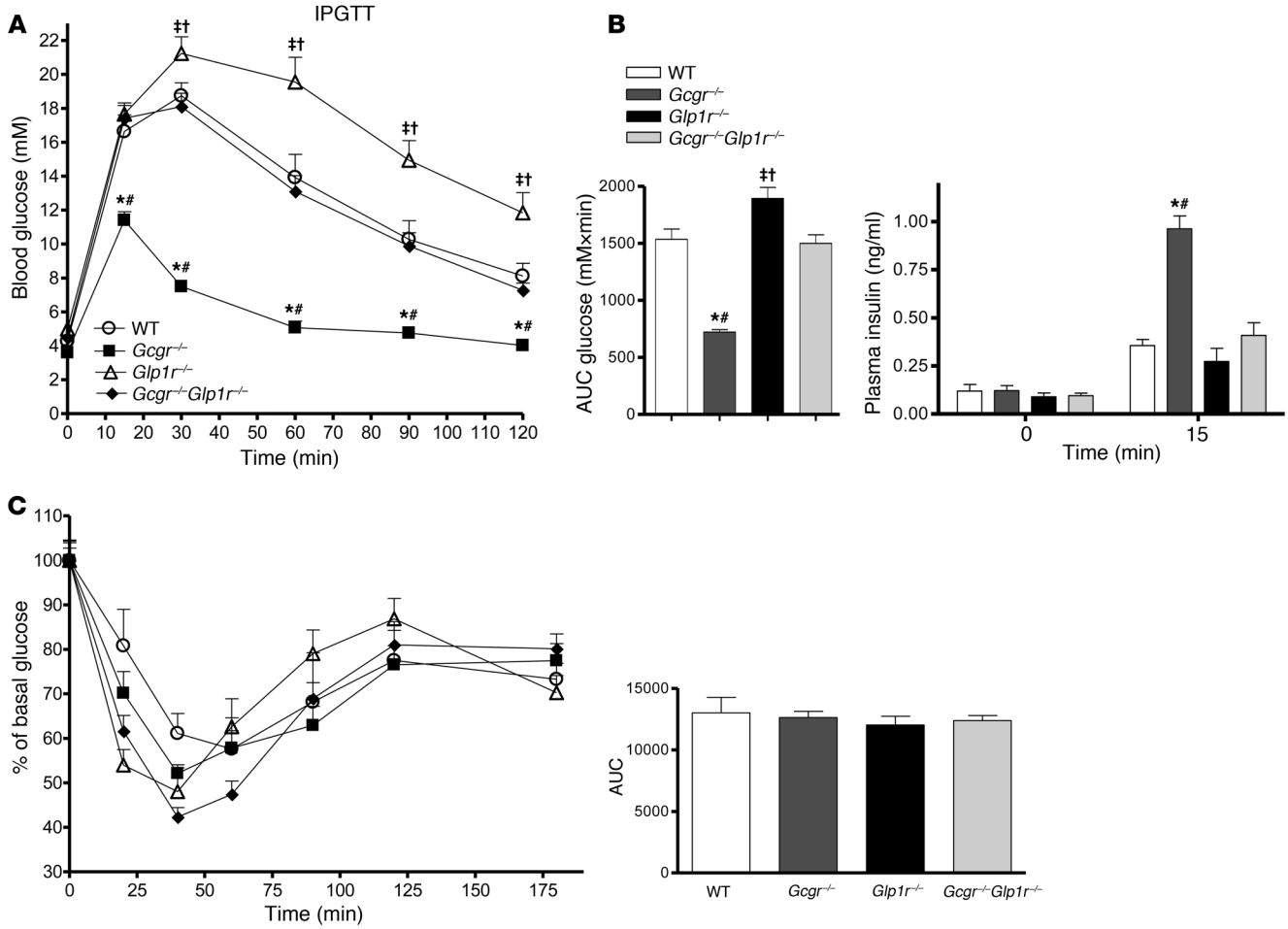

Figure 3

Loss of Glp1r reverses improvements in i.p. glucose tolerance without altering insulin sensitivity in *Gcgr*$^{-/-}$ mice. (**A**) IPGTT in 8- to 10-week-old WT, *Gcgr*$^{-/-}$, *Glp1r*$^{-/-}$, and *Gcgr*$^{-/-}$*Glp1r*$^{-/-}$ mice (n = 9–24 mice per group). (**B**) Area under the curve and plasma insulin levels at 0 and 15 minutes following i.p. glucose challenge (n = 4–8 mice per group). (**C**) Insulin tolerance test in 12- to 14-week-old mice; values are normalized to basal glucose, with right graph showing area under the glucose curve (n = 5–20 mice per group). Values are expressed as mean ± SEM. *P < 0.05, *Gcgr*$^{-/-}$ versus *Gcgr*$^{-/-}$*Glp1r*$^{-/-}$ mice; $^{\#}P$ < 0.05, *Gcgr*$^{-/-}$ versus WT mice; $^{\ddagger}P$ < 0.05, *Glp1r*$^{-/-}$ versus WT mice; $^{\dagger}P$ < 0.05, *Glp1r*$^{-/-}$ versus *Gcgr*$^{-/-}$*Glp1r*$^{-/-}$ mice.

enhanced response to GIP, *Gcgr*$^{-/-}$*Glp1r*$^{-/-}$ islets exhibited a normal response to pituitary adenylate cyclase–activating peptide (PACAP) but significantly reduced insulin secretory responses to tolbutamide and L-arginine (Figure 5B). Consistent with the increased GIP sensitivity demonstrated for insulin secretion (Figure 5A), *Gcgr*$^{-/-}$*Glp1r*$^{-/-}$ islets also exhibited enhanced cAMP accumulation in response to GIP (Figure 5C). To evaluate GIP sensitivity in vivo, we administered i.p. glucose in the presence or absence of submaximal doses of exogenous GIP to WT, *Glp1r*$^{-/-}$, *Gcgr*$^{-/-}$, and *Gcgr*$^{-/-}$*Glp1r*$^{-/-}$ mice. Both *Glp1r*$^{-/-}$ and to a greater extent *Gcgr*$^{-/-}$*Glp1r*$^{-/-}$ mice exhibited enhanced sensitivity to GIP, as revealed by reduced glycemic excursions and increased circulating levels of plasma insulin in response to exogenous GIP administration (Figure 6, A–D, and Supplemental Figure 3, A–D).

Plasticity of the incretin axis revealed through reduction of Gcgr action in Glp1r$^{-/-}$*Gipr*$^{-/-}$ *mice*. The available data strongly suggested that preservation of improved glucose tolerance and enhanced insulin secretion despite loss of GLP-1 action reflects increased GIP sensitivity in *Gcgr*$^{-/-}$*Glp1r*$^{-/-}$ islets. To more rigorously test this hypothesis, we reduced Gcgr expression using ASOs in mice lacking both functional incretin receptors, i.e., *Glp1r*$^{-/-}$*Gipr*$^{-/-}$ (double incretin receptor knockout [DIRKO]) mice (34). Hepatic *Gcgr* mRNA transcripts were markedly decreased and plasma levels of GLP-1 progressively increased in WT and DIRKO mice following ASO treatment (Figure 7, A and B, respectively). WT mice treated with Gcgr ASOs showed improved i.p. glucose tolerance and increased insulin levels following i.p. glucose challenge (Figure 7C). In contrast, DIRKO mice treated with Gcgr ASOs showed no improvement in glucose tolerance or insulin levels following i.p. glucose challenge (Figure 7D), consistent with the importance of the GLP-1R for improved β cell function following reduction of Gcgr expression (21, 22, 32). WT mice treated with Gcgr ASOs also showed improved oral glucose tolerance and significantly higher plasma insulin levels than vehicle-treated controls (Figure 7E). Remarkably, despite loss of both classical incretin receptors, DIRKO mice treated with Gcgr ASOs also exhibited improved oral

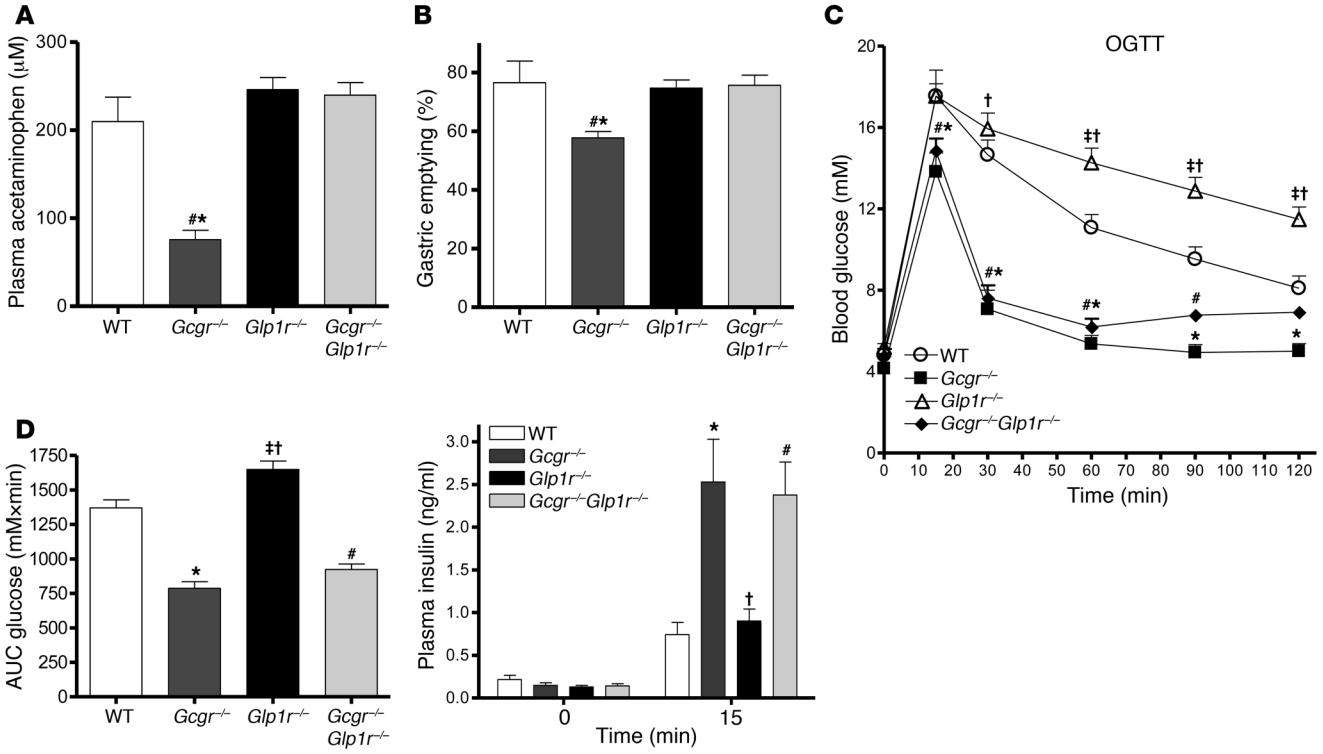

Figure 4

Glp1r mediates reduced gastric emptying but not improved oral glucose tolerance in *Gcgr*$^{-/-}$ mice. (**A**) Liquid-phase gastric emptying (as determined by the appearance of acetaminophen in the circulation after 15 minutes) in 10- to 11-week-old mice (n = 4–14 mice per group). (**B**) Solid-phase gastric emptying in 20-week-old mice (n = 4–10 mice per group). Values are expressed as mean ± SEM. *P < 0.05, *Gcgr*$^{-/-}$ versus *Gcgr*$^{-/-}$*Glp1r*$^{-/-}$ mice; $^{\#}P$ < 0.05, *Gcgr*$^{-/-}$ versus WT mice. (**C**) Blood glucose levels during an OGTT in 10- to 11-week-old mice (n = 11–22 mice per group). (**D**) Area under the glucose curve and plasma insulin levels 0 and 15 minutes following oral glucose challenge (n = 4–9 mice per group). Values are expressed as mean ± SEM. In **C** and **D**: *P < 0.05, *Gcgr*$^{-/-}$ versus WT littermate control mice; $^{\#}P$ < 0.05, *Gcgr*$^{-/-}$*Glp1r*$^{-/-}$ versus WT mice; $^{\dagger}P$ < 0.05, *Glp1r*$^{-/-}$ versus *Gcgr*$^{-/-}$*Glp1r*$^{-/-}$ littermate control mice; $^{\ddagger}P$ < 0.05, *Glp1r*$^{-/-}$ versus WT littermate control mice.

glucose tolerance and significantly increased plasma insulin levels (Figure 7F). Hence, preferential improvement of glucose tolerance and enhanced β cell function following glucose administration in the gut can be achieved despite loss of both incretin receptors.

To identify mechanisms responsible for improvement of oral glucose tolerance and β cell function despite absence of both GLP-1 and GIP receptors, we assessed the expression of insulinotropic receptors in islets from (a) DIRKO mice treated with Gcgr ASOs and (b) *Gcgr*$^{-/-}$*Glp1r*$^{-/-}$ mice. Remarkably, levels of mRNA transcripts for the insulinotropic receptors gastrin-releasing peptide receptor (*Grpr*), *Cckar*, and *Gpr119* were significantly increased in islet RNA from *Gcgr*$^{-/-}$*Glp1r*$^{-/-}$ mice (Figure 8A). Similarly *Gpr119* and *Cckar* mRNA transcripts were also significantly increased in islet RNA from DIRKO mice following Gcgr ASO administration (Figure 8B). These findings raised the possibility that increased activity of related insulinotropic receptors may compensate for the loss of GLP-1 and GIP action on islet β cells.

Gcgr$^{-/-}$*Glp1r*$^{-/-}$ *mice display increased sensitivity to Gpr119 and Cckar agonists*. To assess the functional significance of increased islet receptor expression, we carried out glucose tolerance tests in the presence or absence of exogenous GRP, CCK, PACAP, and the GPR119 agonist AR231453 (35) in WT, *Gcgr*$^{-/-}$, *Glp1r*$^{-/-}$, and *Gcgr*$^{-/-}$*Glp1r*$^{-/-}$ mice. We did not detect enhanced sensitivity to exogenous GRP or PACAP (Supplemental Figure 4 and Supplemental Figure 5, A–D). However, although AR231453 failed to improve i.p. glucose tolerance in WT, *Gcgr*$^{-/-}$, or *Glp1r*$^{-/-}$ mice, a robust improvement in glucose tolerance and marked stimulation of plasma insulin levels were observed following AR231453 administration in *Gcgr*$^{-/-}$*Glp1r*$^{-/-}$ mice (Figure 9, A–D, and Supplemental Figure 6, A–D). Similarly, doses of CCK that failed to improve glucose tolerance in WT or single *Gcgr*$^{-/-}$ or *Glp1r*$^{-/-}$ mice produced a significant reduction in glycemic excursion and significantly elevated plasma insulin levels in *Gcgr*$^{-/-}$*Glp1r*$^{-/-}$ mice, consistent with increased sensitivity to CCK (Figure 10, A–D, and Supplemental Figure 7, A–D).

Discussion

The central importance of glucagon action for the maintenance of euglycemia, together with observations that glucagon secretion may be inappropriately increased in many subjects with T2DM, has fostered great interest in reduction of glucagon action for the treatment of T2DM. Indeed, multiple therapeutic modalities, including insulin, amylin analogs, GLP-1R agonists, and dipeptidyl peptidase–4 inhibitors, exert their anti-diabetic actions in part through suppression of glucagon secretion (36). The *Gcgr*$^{-/-}$ phenotype — healthy mice with reduced fasting and postprandial glycemia (25), resistance to diet-induced obesity, and enhanced β cell function and survival (26) — further sup-

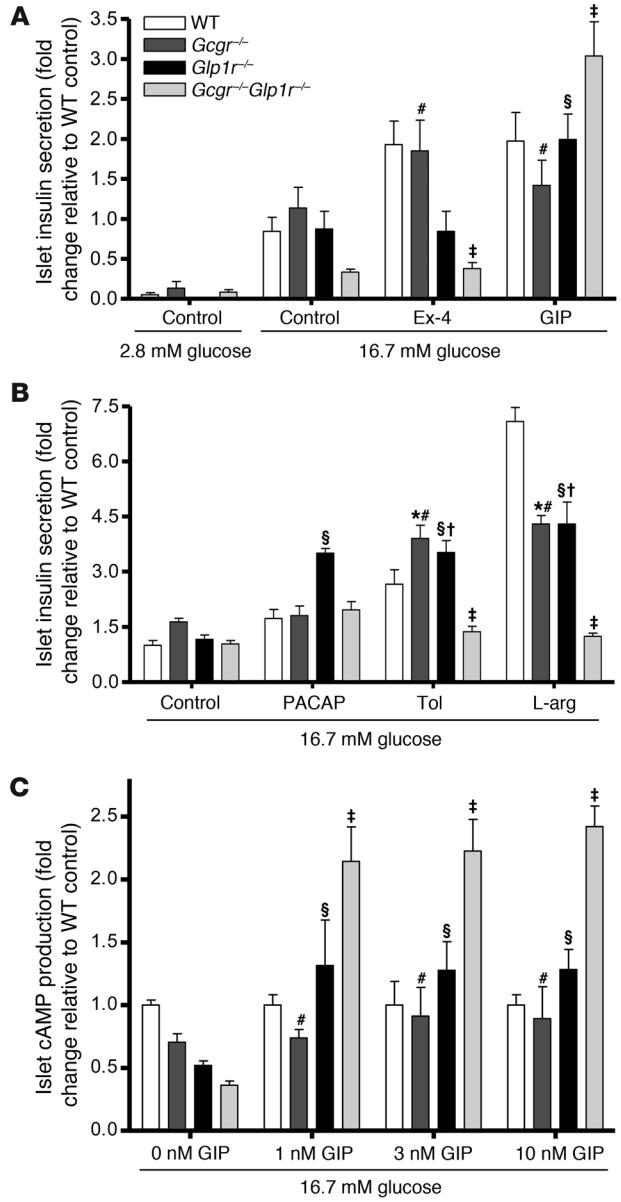

Figure 5
Function of GPCRs in isolated islets. Islet insulin secretion was assessed by preincubation of islets in KRB for 60 minutes at 2.8 mM glucose at 37°C before distribution in batches of 10 islets per condition into wells containing 16.7 mM glucose with or without (**A**) exendin-4 (Ex-4, 10 nM), [D-Ala^2]GIP (GIP, 10 nM), (**B**) PACAP (10 nM), tolbutamide (Tol, 100 μM), or L-arginine (L-arg, 10 mM) for 1 hour at 37°C. Levels of insulin in the secretion medium were normalized to levels of islet insulin content and are expressed as a fold change in insulin secretion relative to WT high-glucose treatment. Insulin content values averaged approximately 30–40 ng/islet for *Glp1r*$^{-/-}$ and WT mice and 15–25 ng/islet for *Gcgr*$^{-/-}$ and *Gcgr*$^{-/-}$*Glp1r*$^{-/-}$ mice (n = 3 mice per group). Data shown are representative of 2–3 independent experiments, each with 3 replicates per condition. (**C**) Total cellular and media cAMP in islets from WT, *Glp1r*$^{-/-}$, *Gcgr*$^{-/-}$, and *Gcgr*$^{-/-}$*Glp1r*$^{-/-}$ mice was quantified following treatment of the islets with 0, 1, 3, or 10 nM [D-Ala^2]GIP. Levels of cAMP in the secretion medium were normalized to levels of islet insulin content and are expressed as a fold change in islet cAMP levels relative to WT high-glucose treatment (n = 3 mice per group). Values are expressed as mean ± SEM. $^{§}P < 0.05$, *Glp1r*$^{-/-}$ versus *Gcgr*$^{-/-}$*Glp1r*$^{-/-}$ mice; $^{\#}P < 0.05$, *Gcgr*$^{-/-}$ versus *Gcgr*$^{-/-}$*Glp1r*$^{-/-}$ mice; $^{‡}P < 0.05$, *Gcgr*$^{-/-}$*Glp1r*$^{-/-}$ versus WT mice; $^{†}P < 0.05$, *Glp1r*$^{-/-}$ versus WT mice; $^{*}P < 0.05$, *Gcgr*$^{-/-}$ versus WT mice.

ports the concept of reducing glucagon receptor signaling for treatment of T2DM. Our studies clearly show that a substantial component of the improved metabolic phenotype of *Gcgr*$^{-/-}$ mice, including control of fasting and fed glycemia, reduced gastric emptying, improved i.p. glucose tolerance, and enhanced β cell function, reflects concomitant upregulation of GLP-1 action in *Gcgr*$^{-/-}$ mice (Figure 11).

Although incretin action classically controls postprandial glucose excursion, considerable evidence supports a role for GLP-1 in the regulation of fasting glucose. GLP-1 receptor agonists reduce fasting glucose in human subjects, in association with reduced levels of circulating glucagon (37). Moreover, the GLP-1R antagonist exendin$_{9-39}$ increases fasting glucose and glucagon levels in baboons (38), and genetic disruption of the Glp1r is associated with fasting hyperglycemia in *Glp1r*$^{-/-}$ mice, without detectable changes in levels of fasting glucagon (32). Surprisingly, elimination of GLP-1 action significantly increased fasting glycemia in *Gcgr*$^{-/-}$*Glp1r*$^{-/-}$ mice. These observations further demonstrate that GLP-1R–dependent pathways may regulate fasting glucose independent of glucagon action, perhaps through incompletely understood neural mechanisms (39).

Reduction or loss of Gcgr signaling (22, 25) or resistance to glucagon action (40) leads to hyperplasia of the exocrine and endocrine pancreas. Selective liver-specific deletion of the gene encoding the G protein $G_s\alpha$ generates a similar phenotype characterized by markedly increased levels of glucagon and GLP-1, increased pancreatic mass, and islet hyperplasia (40). Moreover, this constellation of pancreatic abnormalities is reversible, as glucagon replacement in glucagon-deficient *PC2*-knockout mice normalizes a substantial proportion of these pancreatic phenotypes (41). Although GLP-1R activation promotes expansion of islet and pancreatic mass (29, 31), α cell hyperplasia is not generally observed following administration of GLP-1R agonists. Consistent with these findings, our data demonstrate that the Glp1r does not

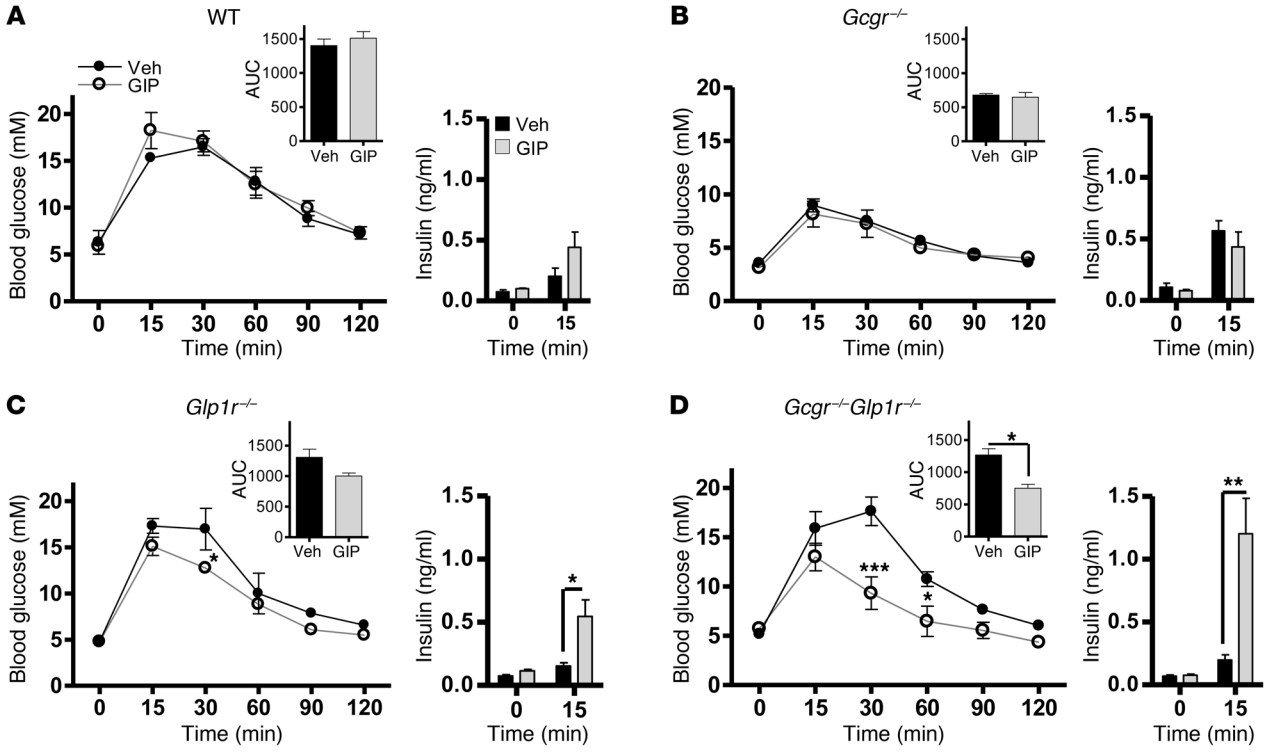

Figure 6

Gcgr$^{-/-}$*Glp1r*$^{-/-}$ mice exhibit enhanced sensitivity to [D-Ala^2]GIP. An IPGTT was performed in 20- to 22-week-old (**A**) WT, (**B**) *Gcgr*$^{-/-}$, (**C**) *Glp1r*$^{-/-}$, and (**D**) *Gcgr*$^{-/-}$*Glp1r*$^{-/-}$ mice following treatment with 1 nmol/kg [D-Ala^2]GIP or saline (vehicle [Veh]). Insets depict the area under the glucose excursion curve (AUC) in mM×min and plasma insulin levels at 0 and 15 minutes following glucose challenge (n = 5–8). Values are expressed as mean ± SEM. *P < 0.05, **P < 0.01, ***P < 0.001, [D-Ala^2]GIP–treated versus saline-treated group.

mediate pancreatic or islet/α cell proliferation in *Gcgr*$^{-/-}$ mice. As *Gcgr*$^{-/-}$ mice are born with normal pancreatic mass and only modest α cell hyperplasia (25, 42), the precise mechanisms linking loss of the Gcgr to marked postnatal expansion of the exocrine and endocrine islet compartments remain unclear.

The finding of reduced gastric emptying in *Gcgr*$^{-/-}$ mice (26) might be explained by enhanced action of multiple proglucagon-derived peptides. GLP-1, oxyntomodulin, and to a lesser extent GLP-2 inhibit gastric emptying (43, 44), and GLP-1 and oxyntomodulin exert their actions on gastric emptying through the GLP-1 receptor. Unexpectedly, however, despite normalization of gastric emptying in *Gcgr*$^{-/-}$*Glp1r*$^{-/-}$ mice, oral glucose tolerance remained substantially improved in *Gcgr*$^{-/-}$*Glp1r*$^{-/-}$ mice, despite elimination of GLP-1R action. Moreover, levels of circulating insulin remained significantly increased following oral glucose challenge despite loss of GLP-1R action in *Gcgr*$^{-/-}$*Glp1r*$^{-/-}$ mice. These findings implicate sustained enhancement of β cell function as a mechanism underlying persistent improvement in oral glucose tolerance despite loss of GLP-1R action in *Gcgr*$^{-/-}$*Glp1r*$^{-/-}$ mice.

The demonstration that the *Gcgr*$^{-/-}$*Glp1r*$^{-/-}$ β cell maintains enhanced insulin secretion in response to oral glucose was unexpected given the previous demonstration of selectively impaired β cell function in *Gcgr*$^{-/-}$ mice compared with age- and sex-matched WT C57BL/6 mice (27) and the multiple lines of evidence supporting important roles for both GLP-1 and glucagon in the control of glucose-stimulated insulin secretion. Glucagon directly stimulates insulin secretion in the rat pancreas independent of GLP-1 receptor action (45), and transgenic Gcgr expression in murine β cells significantly augments glucose-stimulated insulin secretion and reduces random glycemia in RIP-Gcgr transgenic mice (46). Moreover, the glucagon antagonist des-His1-[Glu9]-glucagon-amide significantly reduced glucose-stimulated insulin release in human islets (47). Similarly, GLP-1 induces β cell glucose competence, upregulates insulin biosynthesis and secretion, and markedly enhances glucose sensitivity and glucose-stimulated insulin secretion even in poorly responsive diabetic β cells (48). Hence, given the results of previous observations reporting impaired β cell function in *Gcgr*$^{-/-}$ islets (27), we initially predicted that a further deterioration in β cell function would ensue following removal of the GLP-1R signaling system in *Gcgr*$^{-/-}$ mice.

Surprisingly, however, elimination of Glp1r in *Gcgr*$^{-/-}$ mice did not lead to deterioration in glycemic excursion after oral glucose loading in *Gcgr*$^{-/-}$*Glp1r*$^{-/-}$ mice. The preferential preservation of improved oral glucose tolerance and enhanced insulin secretion following glucose administration via the gastrointestinal tract, despite functional elimination of both the Gcgr and Glp1r, strongly implicates the existence of one or more gut-derived compensatory factors that augment β cell function in an "incretin-like" manner in *Gcgr*$^{-/-}$*Glp1r*$^{-/-}$ mice. As compensatory upregulation of GIP action has been described in *Glp1r*$^{-/-}$ mice, we postulated that upregulation of the GIP-*Gipr* axis might similarly explain preservation of improved oral glucose tolerance in mice following loss of glucagon and GLP-1 action. Although circulating levels of GIP and levels of GIP RNA transcripts were

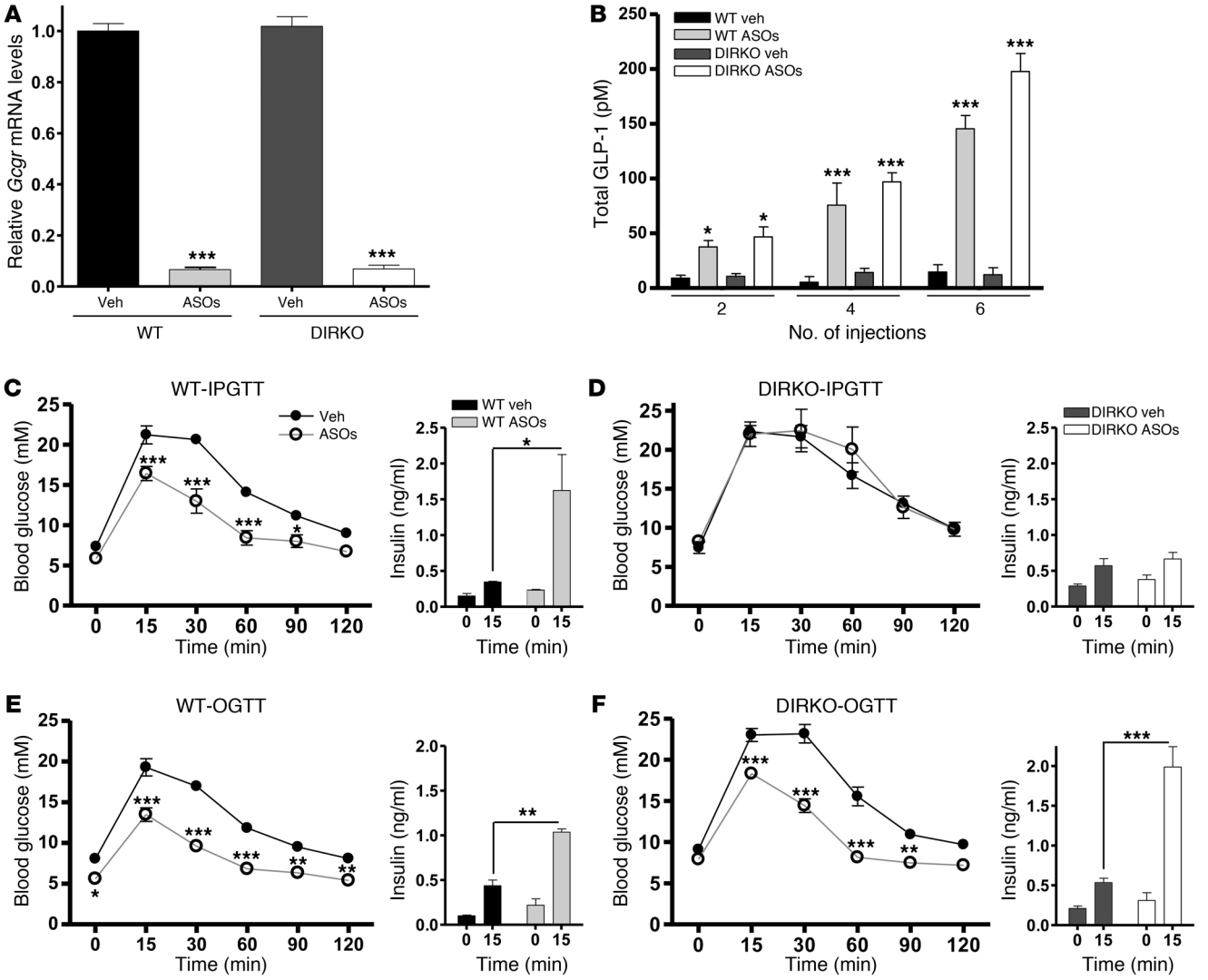

Figure 7

Enteroinsular axis is maintained in DIRKO mice treated with Gcgr ASOs. (**A**) mRNA expression of *Gcgr* in the liver ($n = 3$ per group) following treatment with 6 injections of 25 mg/kg Gcgr ASOs. (**B**) Total plasma GLP-1 levels following 2, 4, or 6 injections of 25 mg/kg saline or Gcgr ASOs ($n = 5$ per group). (**C** and **D**) An i.p. glucose challenge was performed on 13- to 14-week-old male (**C**) WT mice and (**D**) DIRKO mice that had been treated with 3 injections of vehicle or 25 mg/kg Gcgr ASOs ($n = 5$ per group). (**E** and **F**) An OGTT was performed on 15- to 16-week-old (**E**) WT mice and (**F**) DIRKO mice that had been treated with 4 injections of vehicle or 25 mg/kg Gcgr ASOs ($n = 5$ per group). Insets depict plasma insulin levels at 0 and 15 minutes following glucose challenge for saline- or Gcgr ASO–treated mice ($n = 5$ per treatment group). Values are expressed as mean ± SEM. $^*P < 0.05$, $^{**}P < 0.01$, $^{***}P < 0.001$, vehicle- versus Gcgr ASO–treated WT or DIRKO mice.

not increased in islets from *Gcgr*$^{-/-}$*Glp1r*$^{-/-}$ mice, we detected increased insulin secretion and enhanced cAMP accumulation following treatment of *Gcgr*$^{-/-}$*Glp1r*$^{-/-}$ islets with GIP, consistent with increased GIP sensitivity. Furthermore, glucose tolerance was significantly improved and plasma insulin levels were markedly increased following administration of GIP in vivo, further supporting enhanced sensitivity to GIP as a compensatory mechanism augmenting β cell function in *Gcgr*$^{-/-}$*Glp1r*$^{-/-}$ mice.

Unexpectedly, however, we continued to observe preferential improvement of oral glucose tolerance and β cell function in DIRKO mice treated with ASOs to reduce Gcgr expression, implying the existence of additional incretin-like mechanisms compensating for the lack of insulinotropic activity normally subserved by the glucagon, GLP-1, and GIP receptors. Our data demonstrating increased islet expression and functional activity of *Cckar* and *Gpr119* mRNA transcripts from *Gcgr*$^{-/-}$*Glp1r*$^{-/-}$ mice, and in islets from DIRKO mice treated with Gcgr ASOs, reveal a mechanism compensating for the loss of insulinotropic incretin receptors (Figure 11B). The finding of greatly enhanced sensitivity in vivo (improved glucose tolerance and plasma insulin levels) to exogenous ligands for both the *Cckar* and *Gpr119* receptors is consistent with an important role for these receptors in maintaining an incretin response to enteral glucose administration despite loss of GLP-1 and GIP action.

It is notable that the putative ligands for both *Cckar*, namely CCK, and *Gpr119*, principally lipid-derived amides such as oleoyle-

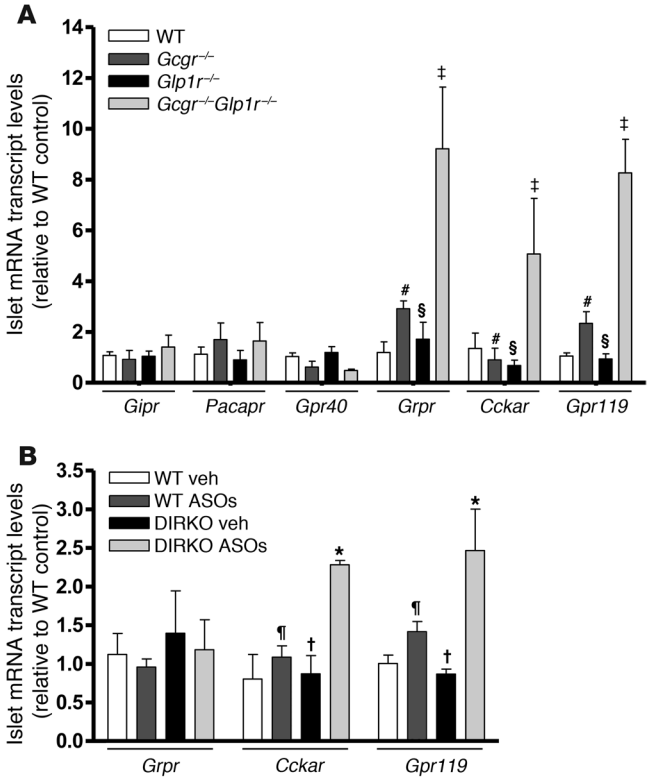

Figure 8
Expression of insulinotropic GPCRs in islets. (**A**) Islets were isolated from WT, *Gcgr*$^{-/-}$, *Glp1r*$^{-/-}$, and *Gcgr*$^{-/-}$*Glp1r*$^{-/-}$ mice, followed by isolation of mRNA for real-time PCR of basal levels of transcripts encoding *Gipr*, *Pacapr*, *Gpr40*, *Grpr*, *Cckar*, and *Gpr119*. (**B**) Islets were isolated from WT or DIRKO mice following 6 injections of vehicle or 25 mg/kg Gcgr ASOs, and mRNA levels of *Grpr*, *Gpr119*, and *Cckar* were determined. Levels of transcripts were normalized to levels of cyclophilin for each RNA sample. $n = 4$ mice per genotype. Values are expressed as mean ± SEM. $^{\S}P < 0.05$, *Glp1r*$^{-/-}$ versus *Gcgr*$^{-/-}$*Glp1r*$^{-/-}$ mice; $^{\#}P < 0.05$, *Gcgr*$^{-/-}$ versus *Gcgr*$^{-/-}$*Glp1r*$^{-/-}$ mice; $^{\ddagger}P < 0.05$, *Gcgr*$^{-/-}$*Glp1r*$^{-/-}$ versus WT mice; $^{\P}P < 0.01$, WT Gcgr ASO–vs DIRKO Gcgr ASO–treated mice; $^{*}P < 0.01$, WT saline- versus DIRKO Gcgr ASO–treated mice; $^{\dagger}P < 0.01$, DIRKO saline- versus DIRKO Gcgr ASO–treated mice.

thanolamide and *N*-oleoyldopamine, would be expected to increase significantly following oral, but not i.p., glucose administration, consistent with our findings of enhanced oral, but not i.p., glucose clearance in *Gcgr*$^{-/-}$*Glp1r*$^{-/-}$ mice. Intriguingly, β cells from DIRKO mice appeared to compensate for loss of incretin receptor and Gcgr expression by similar induction of *Cckar* and *Gpr119* expression, extending the findings of islet incretin receptor plasticity to a second related, yet genetically distinct model.

Studies of islet adaptation classically carried out in the context of β cell injury and regeneration, pregnancy, or high-fat feeding have revealed numerous changes in islet gene expression thought to be linked to the need to expand β cell mass and/or enhance β cell function in response to insulin resistance (49–51). Hence, the concept of β cell plasticity is reasonably well established under physiological conditions requiring enhanced functional β cell mass. There is considerably less information concerning the potential plasticity of the gut-islet axis in circumstances associated with impairment or disruption of classic incretin receptor signals normally emanating from the GLP-1 and GIP receptors. Our observations made using two distinct genetic models, the *Gcgr*$^{-/-}$*Glp1r*$^{-/-}$ mouse and the DIRKO mouse treated with Gcgr ASOs, reveal a heretofore unrecognized capacity for β cell adaptation to loss of insulinotropic receptor signaling (Figure 11). Intriguingly, upregulation of *Cckar* and *Gpr119* expression was also observed in murine islets from pregnant mice, although the functional importance of these findings was not ascertained (51). Our findings may explain why the metabolic phenotype arising from loss of one or both incretin receptors is comparatively mild (32, 34, 52) and identify new models for exploring the expanding importance of incretin-related mechanisms that potentiate β cell function following oral nutrient ingestion.

Methods

Animal studies. *Gcgr*$^{-/-}$*Glp1r*$^{-/-}$ double knockout (DKO) mice were generated by crossing double heterozygote *Glp1r*$^{+/-}$ and *Gcgr*$^{+/-}$ mice to obtain littermate *Gcgr*$^{+/+}$*Glp1r*$^{+/+}$ (WT), *Gcgr*$^{-/-}$ and *Glp1r*$^{-/-}$ single knockouts, and *Gcgr*$^{-/-}$*Glp1r*$^{-/-}$ DKO mice. *Gipr*$^{-/-}$ mice (34) were provided by Y. Seino (Kansai Electric Power Hospital, Osaka, Japan) and used to generate DIRKO mice as previously described (52). All mice used in these studies were male and were housed up to 5 per cage under a light/dark cycle of 12 hours in the Toronto Centre for Phenogenomics animal facility, with free access to food and water except where noted. All procedures were conducted according to protocols and guidelines approved by the Toronto Centre for Phenogenomics Animal Care Committee. For confirmation of genotypes, genomic DNA prepared from tail snips was analyzed by PCR and Southern blotting as described previously (25, 32).

Treatment of mice with Gcgr ASOs. DIRKO and WT mice (11–13 weeks old) were given subcutaneous injections of Gcgr ASOs (Sigma-Aldrich, ISIS 180475, hybridizes to bases 1348–1367 of mouse GCGR sequence NM 008101.1 and bases 1398–1417 of rat GCGR sequence M96674.1) at a dose of 25 mg/kg every 3.5 days for a maximum of 6 injections (22). Intraperitoneal glucose tolerance tests (IPGTTs) were performed after administration of 3 injections of the ASOs, and oral glucose tolerance tests (OGTTs) were performed after administration of 4 injections of the ASOs. Mice were euthanized after administration of 6 injections of the ASOs, and islets and livers were obtained and examined for gene expression. DIRKO and WT mice treated with the Gcgr ASOs were fasted for 6 hours prior to the glucose tolerance tests.

Treatment of mice with peptides and agonists. *Gcgr*$^{-/-}$*Glp1r*$^{-/-}$ mice and littermate controls were treated orally 30 minutes prior to IPGTT with vehicle (80% polyethylene glycol (PEG) 400, 10% Tween 80, and 10% ethanol) or the *Gpr119* agonist AR231453 (5 mg/kg and 20 mg/kg, Arena Pharmaceuticals) (35). *Gcgr*$^{-/-}$*Glp1r*$^{-/-}$ mice and littermate controls were injected

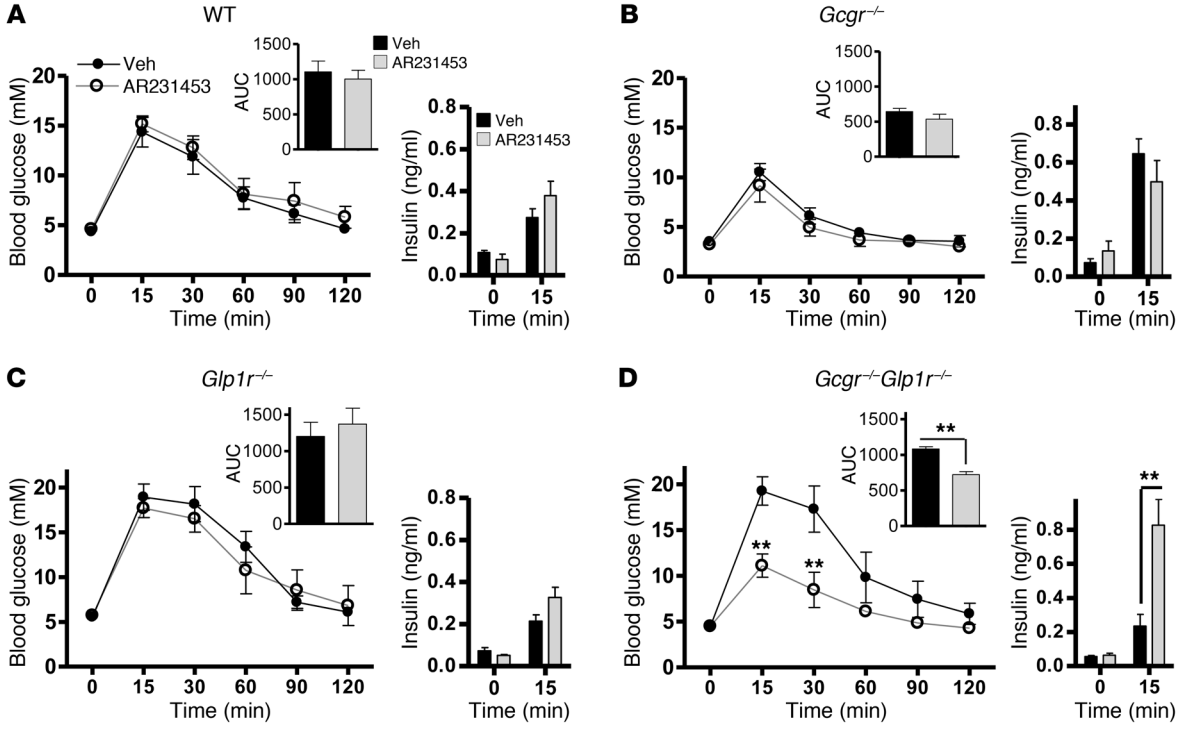

Figure 9

Gcgr$^{-/-}$*Glp1r*$^{-/-}$ mice exhibit enhanced sensitivity to the GPR119 agonist AR231453. An IPGTT was performed in 22- to 24-week-old (**A**) WT (**B**), *Gcgr*$^{-/-}$ (**C**), *Glp1r*$^{-/-}$, and (**D**) *Gcgr*$^{-/-}$*Glp1r*$^{-/-}$ mice 30 minutes following treatment with 5 mg/kg AR231453 or vehicle. Insets depict the area under the glucose excursion curve in mM.min and plasma insulin levels at 0 and 15 minutes following glucose challenge (n = 5–8). Values are expressed as mean ± SEM. $^{**}P < 0.01$, AR231453- versus vehicle-treated mice.

i.p. with PBS vehicle, [D-ALA^2]GIP (1 or 2 nmol/kg) (CHI Scientific), GRP (20 nmol/kg) (Bachem), CCK-8 (9 μg/kg or 18 μg/kg), or PACAP-38 (1.3 nmol/kg), immediately prior to IPGTT (Sigma-Aldrich).

Assessment of food intake. Sixteen- to 18 week-old mice were fasted overnight (16–18 hours), weighed, and then placed in individual cages containing pre-weighed rodent chow, with free access to water. Food was reweighed after 1, 2, 4, 8, and 24 hours, and food intake was expressed as grams consumed per gram of body weight.

Indirect calorimetry. Eight- to 10-week-old mice were placed in individual metabolic chambers, with free access to food and water. Oxygen consumption, CO_2 production, and total and ambulatory activity were determined by indirect calorimetry using an Oxymax System (Columbus Instruments) as described previously (34).

Pancreas weight and histological analysis. Pancreata from 20- to 24-week-old male mice were weighed, fixed in 10% neutral buffered formalin solution for 48 hours, and then embedded in paraffin. For assessment of islet area and histology, pancreatic sections were immunostained for insulin and/or glucagon, followed by scanning using the ScanScope CS system (Aperio Technologies) at ×20 magnification (53). Digital images were analyzed with ScanScope software (Aperio Technologies). Percent islet area was calculated as the sum of the total cross-sectional area of β and α cells/total pancreas area multiplied by 100.

Glucose tolerance and measurement of plasma metabolites. Eight- to 11-week-old male mice were fasted overnight (16–18 hours), and glucose (1.5 mg/g body weight) was administered orally (through a gavage tube) or via injection into the peritoneal cavity (IPGTT). Blood samples were drawn from the tail vein at 0, 15, 30, 60, 90, and 120 minutes after glucose administration, and blood glucose levels were measured using a Glucometer Elite blood glucose meter (Ascensia; Bayer HealthCare). For plasma insulin determinations, blood samples (100 μl) were drawn from the tail vein during the 0- and 15-minute time periods following glucose administration in a heparinized tube. Plasma was separated by centrifugation at 4°C and stored at –80°C until assayed. Plasma was assayed for insulin using a mouse insulin ELISA kit (Alpco). Plasma GLP-1 levels were measured using a mouse/rat total GLP-1 assay kit (Meso Scale Discovery). Plasma GIP levels were assessed using a mouse/rat total GIP ELISA kit (Linco). Plasma GLP-2 levels were assessed using a mouse/rat total GLP-2 assay kit (Alpco). Plasma levels of active GLP-1 and glucagon were measured using a mouse Milliplex endocrine assay (Millipore).

Insulin tolerance test. Twelve- to 13-week-old male mice were fasted for 5 hours and given 0.7 U/kg insulin (Humulin R, 100 U/ml; Lilly) by i.p. injection. Blood samples for blood glucose determination were drawn from the tail vein at 0, 20, 40, 60, 90, 120, and 180 minutes following insulin administration.

Gastric emptying. Gastric emptying was assessed using two protocols. For measurement of solid-phase gastric emptying, 12-week-old mice were fasted in individual cages overnight (16 hours) and allowed access to a premeasured amount of rodent chow for 1 hour. Food intake was determined by reweighing the rodent chow after 1 hour of refeeding. The stomach was isolated and gastric contents retrieved and weighed. The gastric emptying was determined using the following calculation: gastric emptying (%) = (1 – [stomach content wet weight/food intake]) × 100 (as described previously; ref. 4). In the second protocol, liquid-phase gastric emptying was assessed using the acetaminophen absorption test (54). Ten- to 11-week-old mice were fasted overnight and administered a solution containing acetaminophen at a dose of 100 mg/kg by gavage. Tail vein blood (50 μl) was collected into heparinized tubes at 0 and 15 minutes after acetaminophen

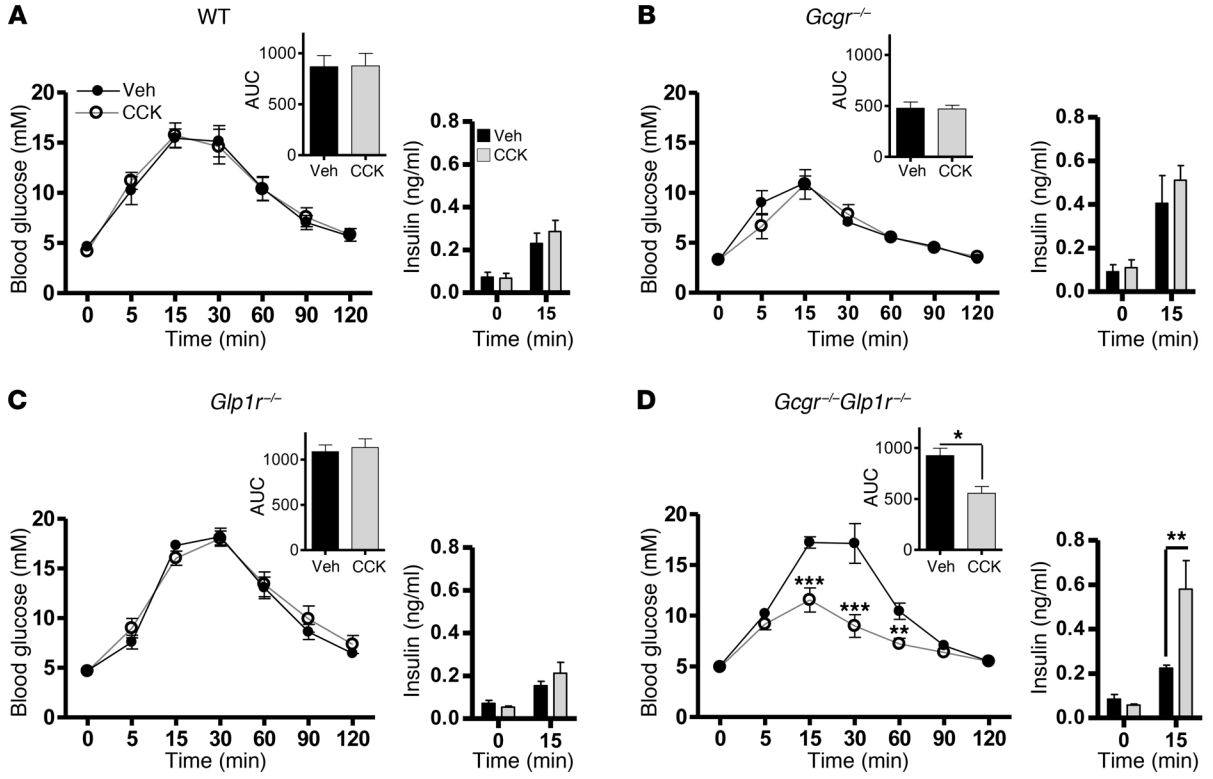

Figure 10

Gcgr$^{-/-}$*Glp1r*$^{-/-}$ mice exhibit increased sensitivity to CCK. An IPGTT was performed in 22- to 24-week-old (**A**) WT, (**B**) *Gcgr*$^{-/-}$, (**C**) *Glp1r*$^{-/-}$, and (**D**) *Gcgr*$^{-/-}$*Glp1r*$^{-/-}$ mice following treatment with 9 μg/kg of CCK-8 or vehicle. Insets depict the area under the glucose excursion curve (AUC) in mM.min and plasma insulin levels at 0 and 15 minutes following glucose challenge (n = 5–8). Values are expressed as mean ± SEM. *P < 0.05, **P < 0.01, ***P <0.001, CCK-8– versus saline-treated mice.

administration. Plasma was separated by centrifugation at 4°C and stored at –20°C until measurement of acetaminophen levels using an enzymatic-spectrophotometric assay (Diagnostic Chemicals Ltd.).

Islet isolation. After CO_2 euthanasia, pancreata from mice were inflated via the pancreatic duct with collagenase type V (0.7 mg/ml in HBSS), excised, and digested at 37°C for 10–15 minutes. The resulting digest was washed twice with cold HBSS (containing 0.25% wt/vol BSA), and islets were separated using a Histopaque density gradient (Sigma-Aldrich). The interface containing islets was removed and washed with HBSS plus BSA, and islets were resuspended in RPMI medium containing 10% FBS, 2 mM L-glutamine, 11 mM glucose, 100 U/ml penicillin, and 100 μg/ml streptomycin. After 4 hours of incubation at 37°C, islets were handpicked into fresh RPMI (containing 5.6 mM glucose) and allowed to recover overnight. Islets with preserved architectural integrity were either used for insulin secretion experiments or washed twice in PBS before being lysed by QIAshredder columns for RNA extraction using the RNeasy Micro Kit (QIAGEN). For insulin secretion, islets were preincubated in Krebs-Ringer buffer (KRB) containing 0.1% BSA, 10 mM HEPES (pH 7.4), and 2.8 mM glucose for 60 minutes. Batches of 10 islets were distributed into wells containing 0.5 ml KRB with either 2.8 or 16.7 mM glucose, with or without [D-Ala^2]GIP, L-arginine, PACAP, tolbutamide, or exendin-4 at the indicated concentrations. After incubation for 1 hour at 37°C, secretion medium was collected and stored at –20°C for assessment of insulin secretion. Islet insulin was extracted by transfer of islets to cold acid-ethanol solution (70% ethanol, 0.18 M HCl) and brief sonication (10 seconds). Insulin levels in secretion media and islet extracts was measured by RIA (Millipore). For cAMP studies, batches of 10 islets were distributed into wells containing 0.5 ml KRB with 16.7 mM glucose, with or without 1, 3, or 10 nM [D-Ala^2]GIP for 1 hour at 37°C. Reactions were terminated by the addition ice-cold absolute ethanol, and cell extracts were collected and stored at –80°C until measurement of cAMP using a cAMP RIA kit according to the manufacturer's instructions (Biomedical Technologies). cAMP levels were normalized to insulin content.

Gut RNA isolation. For gut mRNA analyses, 16- to 18-week-old mice were fasted in individual cages overnight (16 hours) and allowed access to a premeasured amount of rodent chow for 1 hour. Subsequently, duodenums were isolated and snap frozen. RNA isolation was carried out using TRIzol extraction (Invitrogen).

RNA analyses. Following RNA isolation, first-strand complementary DNA was synthesized from total RNA using the SuperScript III reverse transcriptase synthesis system (Invitrogen) and random hexamers. Real-time PCR was performed with the ABI Prism 7900 Sequence Detection System using TaqMan Gene Expression Assays and TaqMan Universal PCR Master Mix (Applied Biosystems). Levels of RNA transcripts were quantified using the $2^{-\Delta\Delta Ct}$ method normalized to peptidyl-propyl isomerase A (cyclophilin).

Statistics. Results are presented as mean ± SEM. Statistical significance was determined using 1-way or 2-way ANOVA with Bonferroni post-hoc tests (as appropriate) using GraphPad Prism 4.0 (GraphPad Software Inc.). Statistical significance was noted when P values were less than 0.05.

Acknowledgments

We would like to thank Xiemin Cao for technical assistance with islet experiments and collection of blood samples during glu-

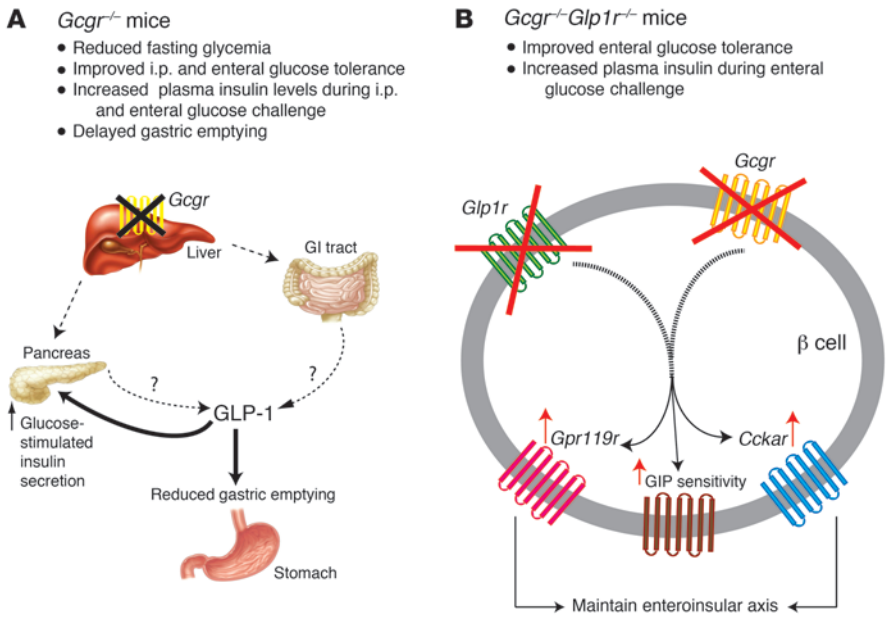

Figure 11
Schematic of proposed model. (**A**) Loss of Gcgr in the liver markedly elevates plasma GLP-1 levels, which promotes glucose-stimulated insulin secretion during i.p. glucose challenge and inhibits gastric emptying in *Gcgr*$^{-/-}$ mice. (**B**) Loss of Glp1r in the *Gcgr*$^{-/-}$ mice results in preservation of the enteroinsular axis via compensatory mechanisms such as upregulation of *Gpr119* and *Cckar* action in β cells, independent of the increase in GIP sensitivity.

cose tolerance tests. This work was supported in part by operating grants from the Canadian Institutes for Health Research (CIHR) MOP 93749 and MOP 82700. D.J. Drucker is supported by a Canada Research Chair in Regulatory Peptides and a Banting and Best Diabetes Centre–Novo Nordisk Chair in Incretin Biology, and S. Ali is supported by a Banting and Best Diabetes Centre Studentship Award.

Received for publication May 6, 2010, and accepted in revised form February 9, 2011.

Address correspondence to: Daniel J. Drucker, Mt. Sinai Hospital SLRI, 600 University Ave TCP5-1004, Toronto, Ontario, Canada M5G 1X5. Phone: 416.361.2661; Fax: 416.361.2669; E-mail: d.drucker@utoronto.ca.

1. Cryer PE. Hypoglycaemia: the limiting factor in the glycaemic management of Type I and Type II diabetes. *Diabetologia*. 2002;45(7):937–948.
2. Jaspan JB, Rubinstein AH. Circulating glucagon: plasma profiles and metabolism in health and disease. *Diabetes*. 1977;26(9):887–902.
3. Unger RH, Aguilar-Parada E, Muller WA, Eisentraut AM. Studies of pancreatic alpha cell function in normal and diabetic subjects. *J Clin Invest*. 1970;49(4):837–848.
4. Sherwin RS, Fisher M, Hendler R, Felig P. Hyperglucagonemia and blood glucose regulation in normal, obese and diabetic subjects. *N Engl J Med*. 1976; 294(9):455–461.
5. Unger RH. Glucagon physiology and pathophysiology in the light of new advances. *Diabetologia*. 1985;28(8):574–578.
6. Campos RV, Lee YC, Drucker DJ. Divergent tissue-specific and developmental expression of receptors for glucagon and glucagon-like peptide-1 in the mouse. *Endocrinology*. 1994;134(5):2156–2164.
7. Marks J, Debnam ES, Dashwood MR, Srai SK, Unwin RJ. Detection of glucagon receptor mRNA in the rat proximal tubule: potential role for glucagon in the control of renal glucose transport. *Clin Sci (Lond)*. 2003;104(3):253–258.
8. Dunphy JL, Taylor RG, Fuller PJ. Tissue distribution of rat glucagon receptor and GLP-1 receptor gene expression. *Mol Cell Endocrinol*. 1998; 141(1–2):179–186.
9. Hansen LH, Abrahamsen N, Nishimura E. Glucagon receptor mRNA distribution in rat tissues. *Peptides*. 1995;16(6):1163–1166.
10. Svoboda M, Tastenoy M, Vertongen P, Robberecht P. Relative quantitative analysis of glucagon receptor mRNA in rat tissues. *Mol Cell Endocrinol*. 1994; 105(2):131–137.
11. Shah P, Basu A, Basu R, Rizza R. Impact of lack of suppression of glucagon on glucose tolerance in humans. *Am J Physiol*. 1999;277(2 pt 1):E283–E290.
12. Consoli A. Role of liver in pathophysiology of NIDDM. *Diabetes Care*. 1992;15(3):430–441.
13. Muller WA, Faloona GR, Aguilar-Parada E, Unger RH. Abnormal alpha-cell function in diabetes. Response to carbohydrate and protein ingestion. *N Engl J Med*. 1970;283(3):109–115.
14. Dinneen S, Alzaid A, Turk D, Rizza R. Failure of glucagon suppression contributes to postprandial hyperglycaemia in IDDM. *Diabetologia*. 1995;38(3):337–343.
15. Jiang G, Zhang BB. Glucagon and regulation of glucose metabolism. *Am J Physiol Endocrinol Metab*. 2003;284(4):E671–E678.
16. Johnson DG, Goebel CU, Hruby VJ, Bregman MD, Trivedi D. Hyperglycemia of diabetic rats decreased by a glucagon receptor antagonist. *Science*. 1982; 215(4536):1115–1116.
17. Brand CL, Rolin B, Jorgensen PN, Svendsen I, Kristensen JS, Holst JJ. Immunoneutralization of endogenous glucagon with monoclonal glucagon antibody normalizes hyperglycaemia in moderately streptozotocin-diabetic rats. *Diabetologia*. 1994; 37(10):985–993.
18. Unson CG, Cypess AM, Wu CR, Goldsmith PK, Merrifield RB, Sakmar TP. Antibodies against specific extracellular epitopes of the glucagon receptor block glucagon binding. *Proc Natl Acad Sci U S A*. 1996; 93(1):310–315.
19. Dallas-Yang Q, et al. Hepatic glucagon receptor binding and glucose-lowering in vivo by peptidyl and non-peptidyl glucagon receptor antagonists. *Eur J Pharmacol*. 2004;501(1–3):225–234.
20. Qureshi SA, et al. A novel glucagon receptor antagonist inhibits glucagon-mediated biological effects. *Diabetes*. 2004;53(12):3267–3273.
21. Liang Y, et al. Reduction in glucagon receptor expression by an antisense oligonucleotide ameliorates diabetic syndrome in db/db mice. *Diabetes*. 2004; 53(2):410–417.
22. Sloop KW, et al. Hepatic and glucagon-like peptide-1-mediated reversal of diabetes by glucagon receptor antisense oligonucleotide inhibitors. *J Clin Invest*. 2004;113(11):1571–1581.
23. Winzell MS, et al. Glucagon receptor antagonism improves islet function in mice with insulin resistance induced by a high-fat diet. *Diabetologia*. 2007; 50(7):1453–1462.
24. Parker JC, Andrews KM, Allen MR, Stock JL, McNeish JD. Glycemic control in mice with targeted disruption of the glucagon receptor gene.

Biochem Biophys Res Commun. 2002;290(2):839–843.
25. Gelling RW, et al. Lower blood glucose, hyperglucagonemia, and pancreatic {alpha} cell hyperplasia in glucagon receptor knockout mice. *Proc Natl Acad Sci U S A*. 2003;100(3):1438–1443.
26. Conarello SL, et al. Glucagon receptor knockout mice are resistant to diet-induced obesity and streptozotocin-mediated beta cell loss and hyperglycaemia. *Diabetologia*. 2007;50(1):142–150.
27. Sorensen H, et al. Glucagon receptor knockout mice display increased insulin sensitivity and impaired {beta}-cell function. *Diabetes*. 2006; 55(12):3463–3469.
28. Pederson RA, et al. Enhanced glucose-dependent insulinotropic polypeptide secretion and insulinotropic action in glucagon-like peptide 1 receptor$^{-/-}$ mice. *Diabetes*. 1998;47(7):1046–1052.
29. Baggio LL, Huang Q, Cao X, Drucker DJ. The long-acting albumin-exendin-4 GLP-1R agonist CJC-1134 engages central and peripheral mechanisms regulating glucose homeostasis. *Gastroenterology*. 2008; 134(4):1137–1147.
30. Brubaker PL, Drucker DJ. Glucagon-like peptides regulate cell proliferation and apoptosis in the pancreas, gut and central nervous system. *Endocrinology*. 2004;145(6):2653–2659.
31. Koehler JA, Baggio LL, Lamont BJ, Ali S, Drucker DJ. GLP-1 receptor activation modulates pancreatitis-associated gene expression but does not modify the susceptibility to experimental pancreatitis in mice. *Diabetes*. 2009;58(9):2148–2161.
32. Scrocchi LA, et al. Glucose intolerance but normal satiety in mice with a null mutation in the glucagon-like peptide receptor gene. *Nature Med*. 1996; 2(11):1254–1258.
33. Creutzfeld WO, Kleine N, Willms B, Orskov C, Holst JJ, Nauck MA. Glucagonostatic actions and reduction of fasting hyperglycemia by exogenous glucagon-like peptide I(7-36) amide in type I diabetic patients. *Diabetes Care*. 1996;19(6):580–586.
34. Hansotia T, et al. Extrapancreatic incretin receptors modulate glucose homeostasis, body weight, and energy expenditure. *J Clin Invest*. 2007;117(1):143–152.
35. Flock G, Holland D, Seino Y, Drucker DJ. *GPR119* regulates murine glucose homeostasis through incretin receptor-dependent and independent mechanisms. *Endocrinology*. 2011;152(2):374–383.
36. Ali S, Drucker DJ. Benefits and limitations of reducing glucagon action for the treatment of type 2 diabetes. *Am J Physiol Endocrinol Metab*. 2009; 296(3):E415–E421.
37. Drucker DJ, Nauck MA. The incretin system: glucagon-like peptide-1 receptor agonists and dipeptidyl peptidase-4 inhibitors in type 2 diabetes. *Lancet*. 2006; 368(9548):1696–1705.
38. D'Alessio DA, et al. Elimination of the action of glucagon-like peptide 1 causes an impairment of glucose tolerance after nutrient ingestion by healthy baboons. *J Clin Invest*. 1996;97(1):133–138.
39. Knauf C, et al. Brain glucagon-like peptide 1 signaling controls the onset of high-fat diet-induced insulin resistance and reduces energy expenditure. *Endocrinology*. 2008;149(10):4768–4777.
40. Chen M, et al. Increased glucose tolerance and reduced adiposity in the absence of fasting hypoglycemia in mice with liver-specific G(s)alpha deficiency. *J Clin Invest*. 2005;115(11):3217–3227.
41. Webb GC, Akbar MS, Zhao C, Swift HH, Steiner DF. Glucagon replacement via micro-osmotic pump corrects hypoglycemia and alpha-cell hyperplasia in prohormone convertase 2 knockout mice. *Diabetes*. 2002; 51(2):398–405.
42. Vuguin PM, et al. Ablation of the glucagon receptor gene increases fetal lethality and produces alterations in islet development and maturation. *Endocrinology*. 2006;147(9):3995–4006.
43. Wettergren A, Schjoldager B, Mortensen PE, Myhre J, Christiansen J, Holst JJ. Truncated GLP-1 (proglucagon 78-107-amide) inhibits gastric and pancreatic functions in man. *Dig Dis Sci*. 1993;38(4):665–673.
44. Schjoldager B, Mortensen PE, Myhre J, Christiansen J, Holst JJ. Oxyntomodulin from distal gut. Role in regulation of gastric and pancreatic functions. *Dig Dis Sci*. 1989;34(9):1411–1419.
45. Kawai K, Yokota C, Ohashi S, Watanabe Y, Yamashita K. Evidence that glucagon stimulates insulin secretion through its own receptor in rats. *Diabetologia*. 1995;38(3):274–276.
46. Gelling RW, et al. Pancreatic beta-cell overexpression of the glucagon receptor gene results in enhanced beta-cell function and mass. *Am J Physiol Endocrinol Metab*. 2009;297(3):E695–E707.
47. Huypens P, Ling Z, Pipeleers D, Schuit F. Glucagon receptors on human islet cells contribute to glucose competence of insulin release. *Diabetologia*. 2000; 43(8):1012–1019.
48. Drucker DJ. The biology of incretin hormones. *Cell Metab*. 2006;3(3):153–165.
49. Rieck S, et al. The transcriptional response of the islet to pregnancy in mice. *Mol Endocrinol*. 2009; 23(10):1702–1712.
50. Kim H, et al. Serotonin regulates pancreatic beta cell mass during pregnancy. *Nat Med*. 2010; 16(7):804–808.
51. Layden BT, et al. Regulation of pancreatic islet gene expression in mouse islets by pregnancy. *J Endocrinol*. 2010;207(3):265–279.
52. Miyawaki K, et al. Glucose intolerance caused by a defect in the entero-insular axis: a study in gastric inhibitory polypeptide receptor knockout mice. *Proc Natl Acad Sci U S A*. 1999;96(26):14843–14847.
53. Maida A, Hansotia T, Longuet C, Seino Y, Drucker DJ. Differential importance of GIP versus GLP-1 receptor signaling for beta cell survival in mice. *Gastroenterology*. 2009;137(6):2146–2157.
54. Maida A, Lovshin JA, Baggio LL, Drucker DJ. The glucagon-like peptide-1 receptor agonist oxyntomodulin enhances {beta}-cell function but does not inhibit gastric emptying in mice. *Endocrinology*. 2008; 149(11):5670–5678.

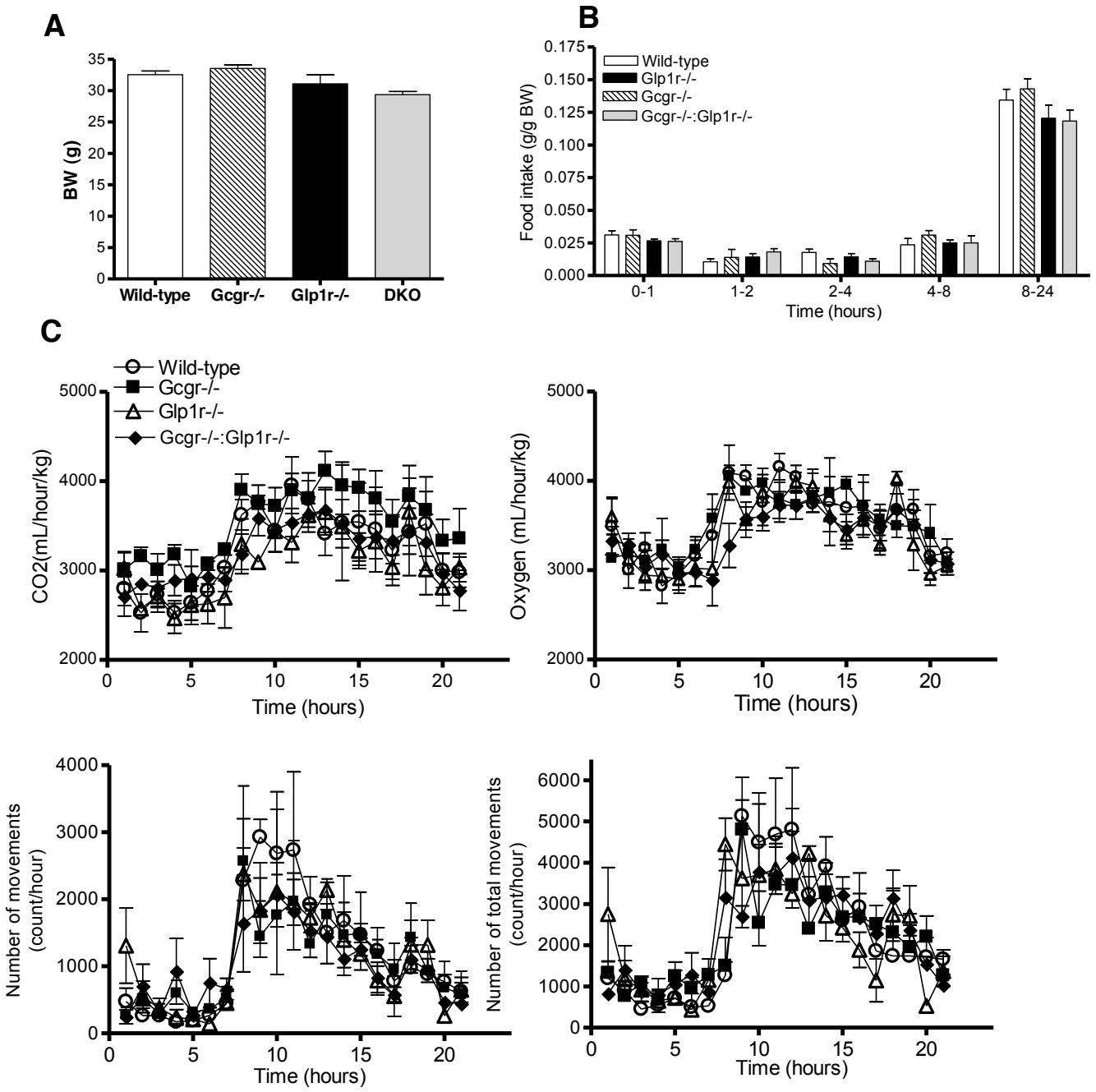

Supplementary Figure 1. Body weight, food intake and energy expenditure. (A) Body weight from 12 week old mice (n = 4-7). (B) Food intake was determined 1, 2, 4, 8 and 24 hours following an overnight fast (n = 4-16). (C) Energy expenditure was determined in 8-10 week old mice. Oxymax measurements were starting at 12pm (n = 6 mice per genotype). Values are expressed as mean ± SEM.

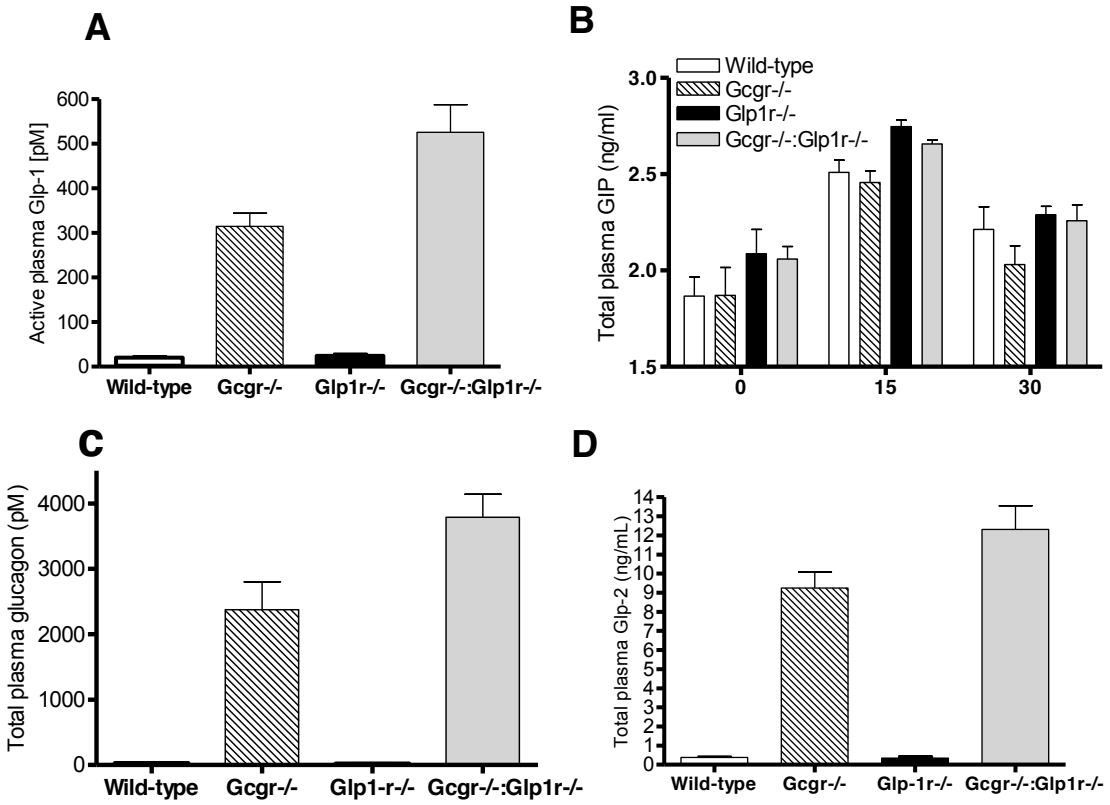

Supplementary Figure 2. ***Plasma levels of total GIP, active GLP-1, total GLP-2 and total Glucagon.*** (A) Random fed active GLP-1 levels in plasma. (B) Plasma levels of total GIP at 0, 15 and 30 min following oral glucose administration. (C) Random fed total glucagon levels in plasma. (D) Random fed total GLP-2 levels in plasma. n=4-10 per genotype. Values are expressed as mean ± SEM.

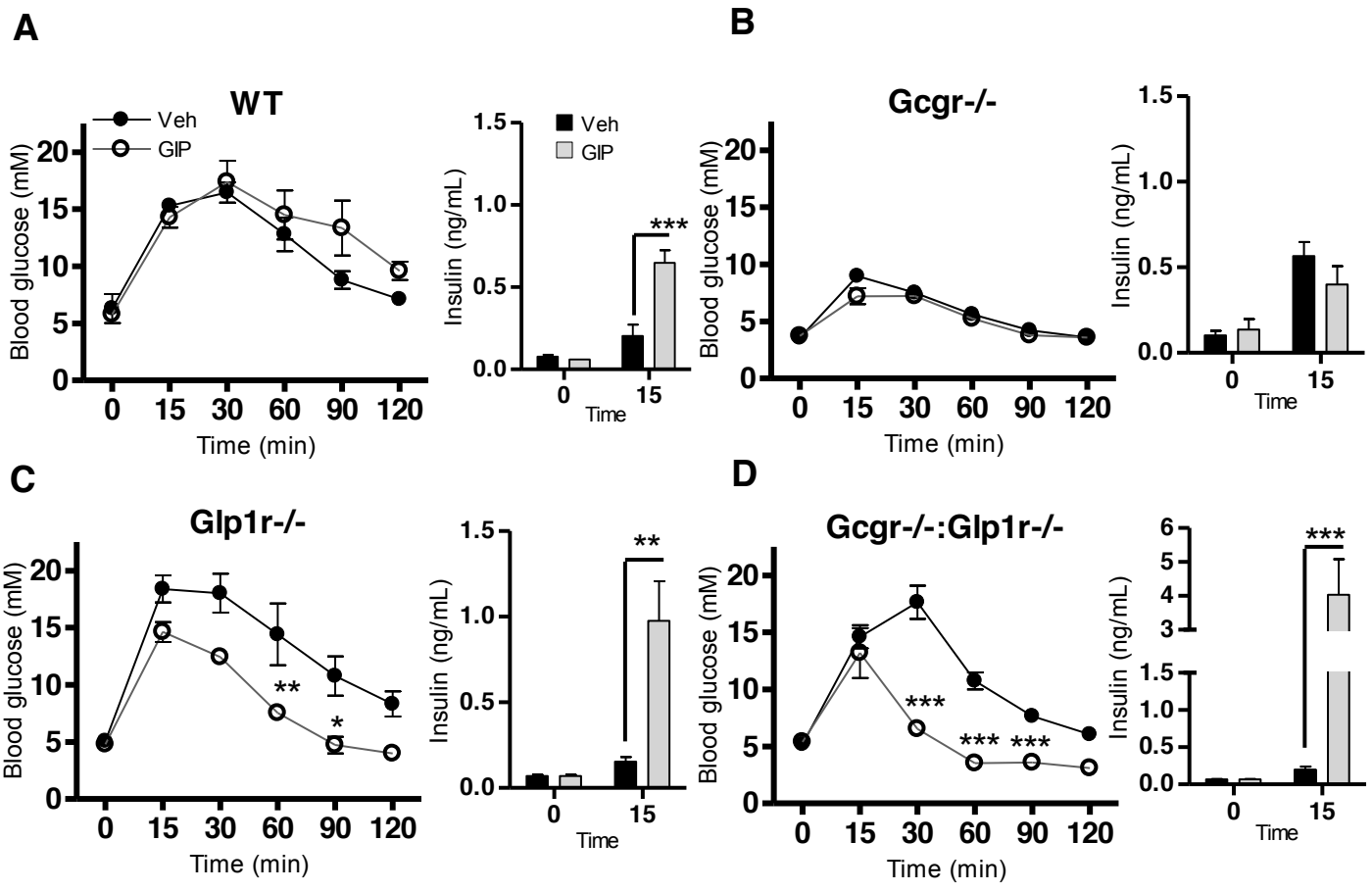

Supplementary Figure 3. ***Gcgr$^{-/-}$:Glp1r$^{-/-}$ mice exhibit enhanced sensitivity to D-Ala$_2$ GIP.*** Intraperitoneal glucose tolerance test was performed in 22-24 week old (A) WT, (B) *Gcgr$^{-/-}$,* (C) G*lp1r$^{-/-}$* ;and (D) *Gcgr$^{-/-}$*:*Glp1r$^{-/-}$* mice immediately following treatment with 2nM of D-Ala$_2$ GIP or saline. Insets depict plasma insulin levels 0 and 15 min following glucose challenge (n = 5-8). Values are expressed as mean ± SEM; **P* < 0.05, ***P <0.01*, *** *P<.001* D-Ala$_{2-}$ vs. vehicle- treated mice.

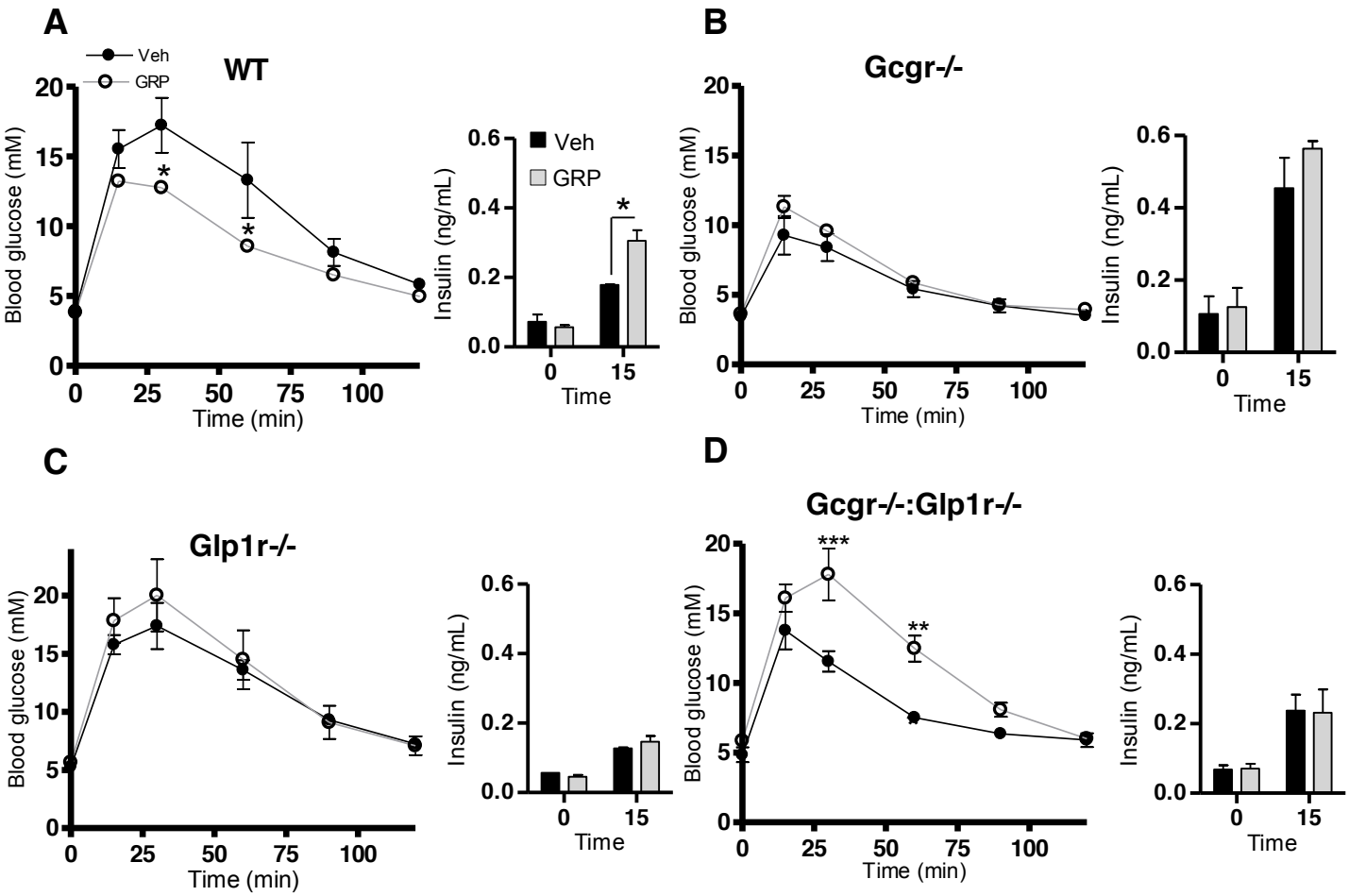

Supplementary Figure 4. ***GRP action in WT and knockout mice.*** Intraperitoneal glucose tolerance test was performed in 22-24 week old (A) WT, (B) *Gcgr*$^{-/-}$, (C) G*lp1r*$^{-/-}$;and (D) *Gcgr*$^{-/-}$:*Glp1r*$^{-/-}$ mice immediately following treatment with 20 nmol/kg of GRP or with saline. Insets depict plasma insulin levels at 0 and 15 min following glucose challenge (n = 5-8). Values are expressed as mean ± SEM; **P* < 0.05, ***P <0.01*, *** *P<.001* GRP- vs. vehicle- treated mice.

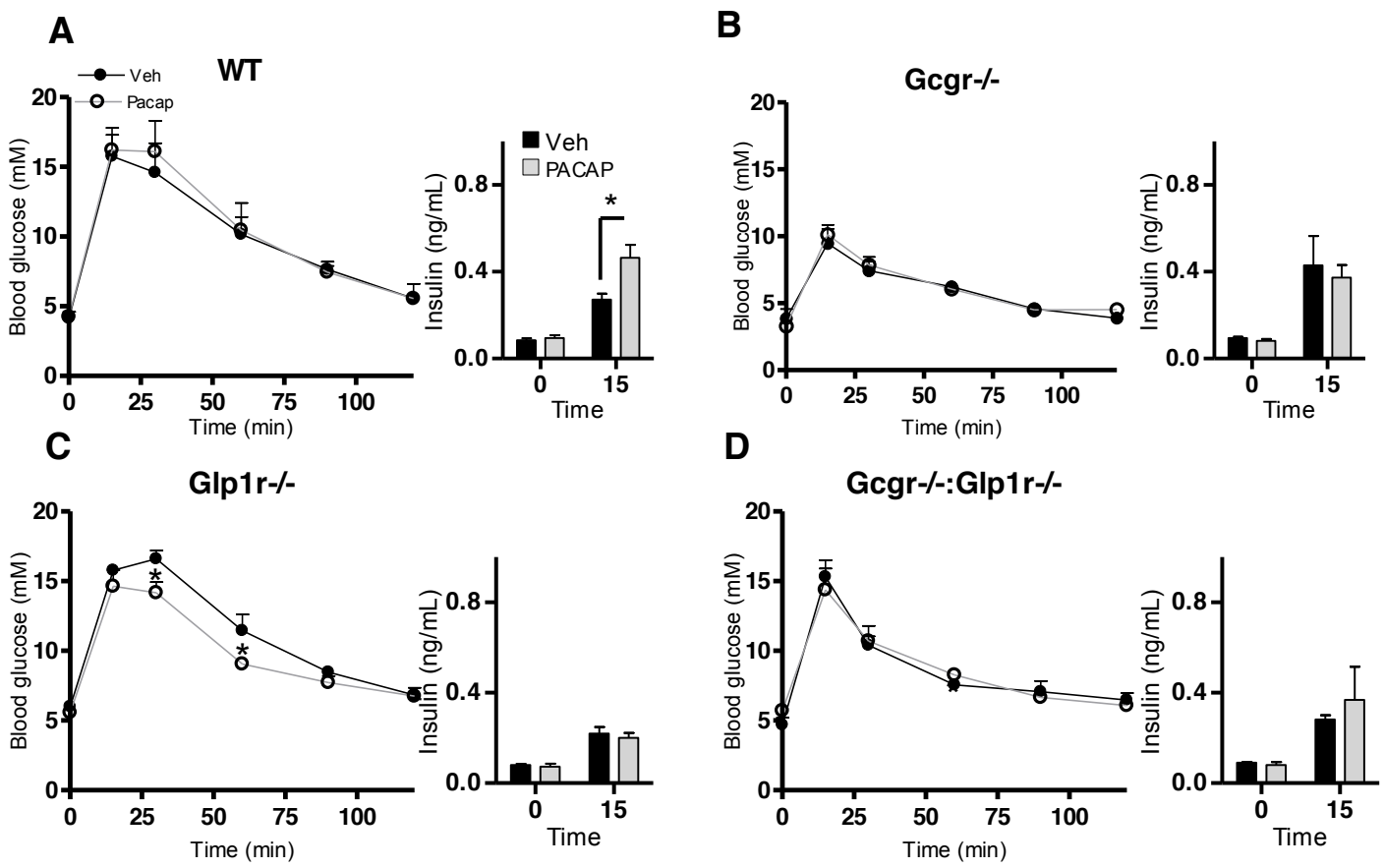

Supplementary Figure 5. ***PACAP action in WT and knockout mice.*** Intraperitoneal glucose tolerance test was performed in 22-24 week old mice A) WT, (B) *Gcgr*$^{-/-}$, (C) G*lp1r*$^{-/-}$;and (D) *Gcgr*$^{-/-}$:*Glp1r*$^{-/-}$ mice immediately following treatment with 1.3 nmol/kg of PACAP-38 or saline. Insets depict plasma insulin levels at 0 and 15 min following glucose challenge (n = 5-8). Values are expressed as mean ± SEM; **P* < 0.05 for PACAP-38- vs. vehicle- treated mice.

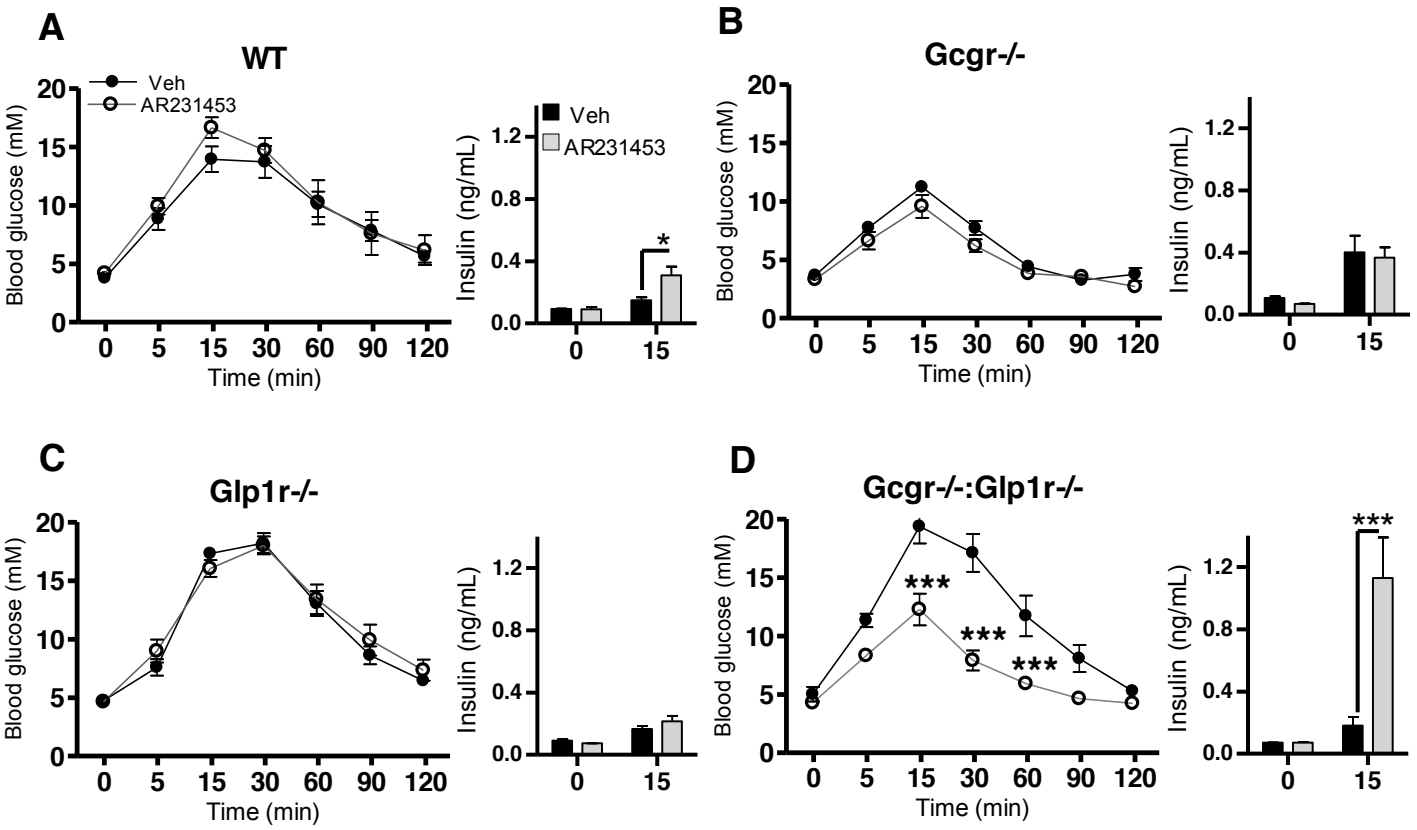

Supplementary Figure 6. Enhanced *sensitivity to the GPR119 agonist AR231453.* An Intraperitoneal glucose tolerance test was performed in 22-24 week old (A) WT, (B) *Gcgr*$^{-/-}$, (C) G*lp1r*$^{-/-}$;and (D) *Gcgr*$^{-/-}$:*Glp1r*$^{-/-}$ mice 30 min following treatment with 20mg/kg of AR231453 or vehicle. Insets depict plasma insulin levels at 0 and 15 min following glucose challenge (n = 5-8). Values are expressed as mean ± SEM; **P* < 0.05, ***P <0.01*, *** *P<.001* AR231453- vs. vehicle- treated mice.

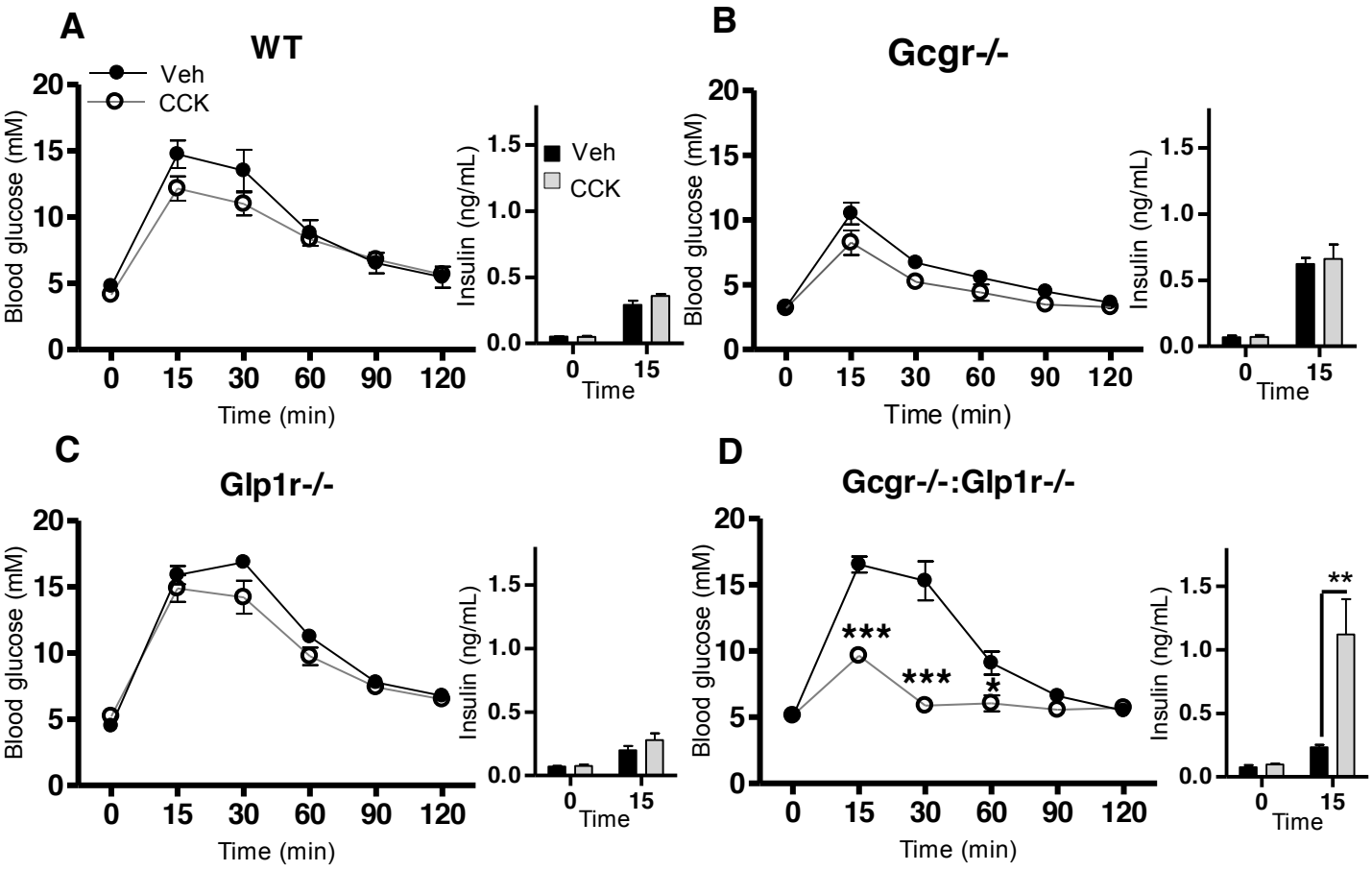

Supplementary Figure 7. Enhanced *sensitivity to CCK.* Intraperitoneal glucose tolerance test was performed in 22-24 week old (A) WT, (B) *Gcgr*$^{-/-}$, (C) G*lp1r*$^{-/-}$;and (D) *Gcgr*$^{-/-}$:*Glp1r*$^{-/-}$ mice immediately following treatment with 18ug/kg of CCK-8 or saline. Insets depict plasma insulin levels at 0 and 15 min following glucose challenge (n = 5-8). Values are expressed as mean ± SEM; **P* < 0.05, ***P <0.01*, *** *P<.001* CCK-8- vs. vehicle- treated mice.

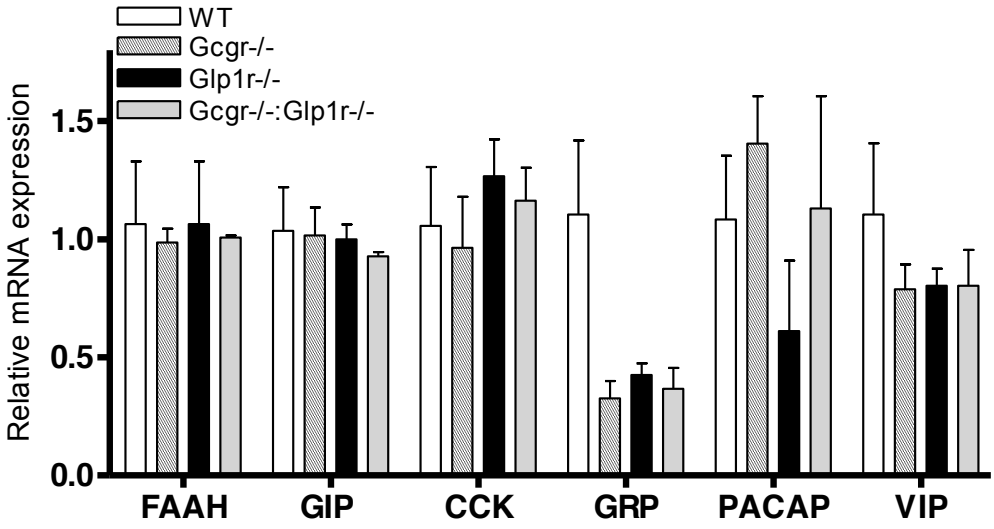

Supplementary Figure 8*. Gut peptide gene expression in re-fed mice*. Duodenums were isolated from *Gcgr-/-*:Glp1r-/-, *Gcgr-/-*, *Glp1r-/-* and WT mice following an overnight fast and refed for 1 hour followed by assessment of basal levels of transcripts encoding FAAH, GIP, CCK, GRP, PACAP and VIP. Levels of transcripts were normalized to levels for cyclophilin for each RNA sample. n = 4 mice per genotype. Values are expressed as mean ± SEM.